







Article

Magnetostructural Properties of Some Doubly-Bridged Phenoxido Copper(II) Complexes

Salah S. Massoud ^{1,2,*} , Febee R. Louka ¹, Madison T. Dial ¹, Nahed N. M. H. Salem ² , Roland C. Fischer ³ , Ana Torvisco ³ , Franz A. Mautner ⁴, Kai Nakashima ⁵, Makoto Handa ⁵  and Masahiro Mikuriya ^{6,*} 

- ¹ Department of Chemistry, University of Louisiana at Lafayette, P.O. Box 43700, Lafayette, LA 70504, USA
² Department of Chemistry, Faculty of Science, Alexandria University, Moharam Bey, Alexandria 21511, Egypt
³ Institut für Anorganische Chemie, Technische Universität Graz, Stremayrgasse 9/V, A-8010 Graz, Austria
⁴ Institut für Physikalische and Theoretische Chemie, Technische Universität Graz, Stremayrgasse 9/II, A-8010 Graz, Austria
⁵ Department of Chemistry, Interdisciplinary Graduate School of Science and Engineering, Shimane University, 1060 Nishikawatsu, Matsue 690-8504, Japan
⁶ Department of Applied Chemistry for Environment, School of Biological and Environmental Sciences, Kwansei Gakuin University, 1 Gakuen Uegahara, Sanda 669-1330, Japan
 * Correspondence: ssmassoud@louisiana.edu (S.S.M.); junpei@kwansei.ac.jp (M.M.); Tel.: +01-337-482-5672 (S.S.M.); +81-79-565-8140 (M.M.)

Abstract: Three new tripod tetradentate phenolate-amines (H_2L^1 , H_2L^4 and H_2L^9), together with seven more already related published ligands, were synthesized, and characterized. With these ligands, two new dinuclear doubly-bridged-phenoxido copper(II) complexes (**3**, **4**), and six more complexes (**1**, **2**, **5–8**), a new trinuclear complex (**9**) with an alternative doubly-bridged-phenoxido and –methoxido, as well as the 1D polymer (**10**) were synthesized, and their molecular structures were characterized by spectroscopic methods and X-ray single crystal crystallography. The Cu(II) centers in these complexes exhibit distorted square-pyramidal arrangement in **1–4**, mixed square pyramidal and square planar in **5**, **6**, and **9**, and distorted octahedral (5+1) arrangements in **7** and **8**. The temperature dependence magnetic susceptibility study over the temperature range 2–300 K revealed moderate–relatively strong antiferromagnetic coupling (AF) ($|J| = 289–145\text{ cm}^{-1}$) in complexes **1–6**, weak-moderate AF ($|J| = 59\text{ cm}^{-1}$) in the trinuclear complex **9**, but weak AF interactions ($|J| = 3.6$ & 4.6 cm^{-1}) were obtained in **7** and **8**. No correlation was found between the exchange coupling J and the geometrical structural parameters of the four-membered Cu_2O_2 rings.

Keywords: copper(II) complexes; phenolate compounds; tripodal ligands; X-ray structures; magnetic properties; computational



Citation: Massoud, S.S.; Louka, F.R.; Dial, M.T.; Salem, N.N.M.H.; Fischer, R.C.; Torvisco, A.; Mautner, F.A.; Nakashima, K.; Handa, M.; Mikuriya, M. Magnetostructural Properties of Some Doubly-Bridged Phenoxido Copper(II) Complexes. *Molecules* **2023**, *28*, 2648. <https://doi.org/10.3390/molecules28062648>

Academic Editor: Takashiro Akitsu

Received: 13 February 2023

Revised: 10 March 2023

Accepted: 10 March 2023

Published: 14 March 2023



Copyright: © 2023 by the authors. Licensee MDPI, Basel, Switzerland. This article is an open access article distributed under the terms and conditions of the Creative Commons Attribution (CC BY) license (<https://creativecommons.org/licenses/by/4.0/>).

1. Introduction

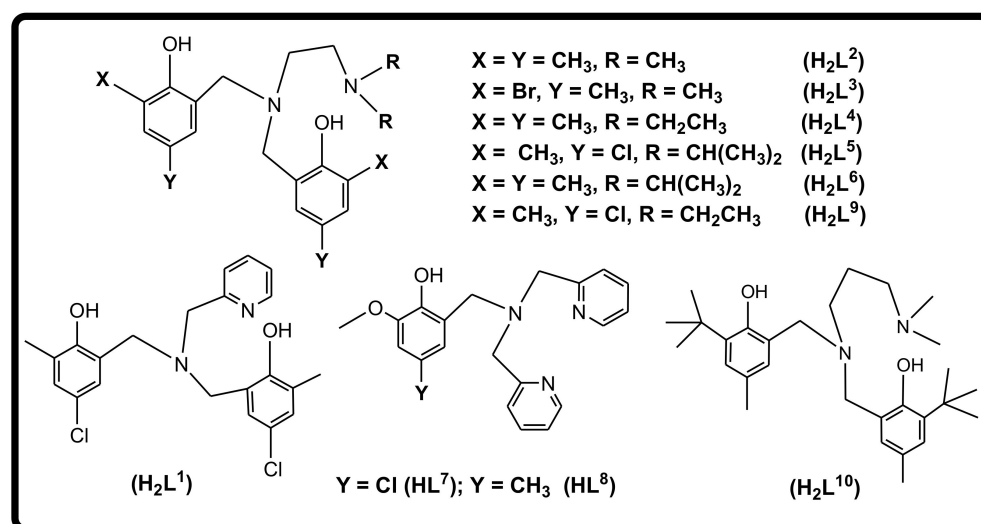
Dinuclear copper(II) complexes in which the Cu(II) ions are bridged by a phenolate oxygen atoms (L-O) and an exogenous bridging atom X with the coordination core $Cu(\mu-L-O)(\mu-X)Cu$ ($X = L-O, OH^-, OR^-, O^{2-}, OAc^-, N_3^-$ and Cl^-) have been reported for a number of ligands with different skeletons frames [1–12]. Some of these complexes have served as cooperative model systems to mimic the active sites in metalloproteins, such as hemocyanin [12–16], metalloenzymes, such as tyrosinase [16–18], galactose oxidase (GOase) [19–24], superoxide dismutase (SOD) [25–27], and as artificial nucleases for promoting the cleavage of DNA [5,6,28,29] as well as anticancer agents [30,31].

The dinuclear copper(II) compounds constructed from the cores $Cu(\mu-L-O)(\mu-X)Cu$ and $Cu(\mu-L-O)_2Cu$ are stable and the two metal ions are located in close proximity, which lead to strong implications regarding their reactivity and magnetic properties due to the interactions between the two paramagnetic Cu(II) centers [32,33]. Different strategies have been employed in the design of this class of compounds. The first approach was

achieved through the interaction Cu(II) salts with tridentate ligand-based phenolates in their skeletons [34–41], and the second approach was via the design of bicompartamental phenolates bearing two pendent arms of N-donor groups [1–6,42,43]. A third approach was also used through the design of tripodal pyridyl tetradentate ligands containing one or two phenolate arms [12,14,15,20,29,44–51].

The structures and magnetic properties of singly-bridged Cu(μ -L-O)Cu and doubly-bridged phenolate Cu(μ -L-O)₂Cu compounds were the subject of numerous investigations [1–4,31,33,34,41,42,44] as well as theoretical studies [31,33,41,51–54]. The energy gap $2J$ arising from the spin singlet-triplet (S-T) state interactions between the two local Cu(II) doublets were evaluated. Many structural parameters were reported to affect the magnitude of the magnetic interactions in the four membered ring, Cu₂O₂ [41,54]. These include the Cu...Cu bond distance and the bridged Cu–O–Cu bond angle [41,54], the geometrical distortion, the dihedral angle between the two copper planes as well as the electronegativity in the bridging phenolate [53]. The presence of electron-withdrawing groups leads to substantial reduction in the antiferromagnetic exchange [53]. The steric effect incorporated into ligand skeleton, which may distort the copper coordination geometry, cannot be ruled out either. The non-covalent bonding interactions (H-bonding, π ... π , stacking interactions, and van der Waals' force) have also been reported to affect the molecular magnetism in these systems [54–62]. In general, strong super exchange antiferromagnetic coupling (AF) was observed in the bridged phenolate compounds [25–27,33,41,43,51–54] but, in a few cases very weak ferromagnetic properties (F) were found [4,22,25,54].

Herein, we describe a general effective procedure for the design of novel series of tripodal phenolate compounds containing pyridyl or aliphatic amine arms with N₃O and N₂O₂ chromophores, where the donor O atoms are provided by one or two phenolate groups (Scheme 1) and their corresponding doubly-bridged phenoxido-Cu(II) complexes. The magnetic properties of the complexes were investigated at variable temperatures and the evaluated exchange coupling constants, J , are discussed in relation to their molecular structures.



Scheme 1. Phenolate ligands used in this study and their abbreviations.

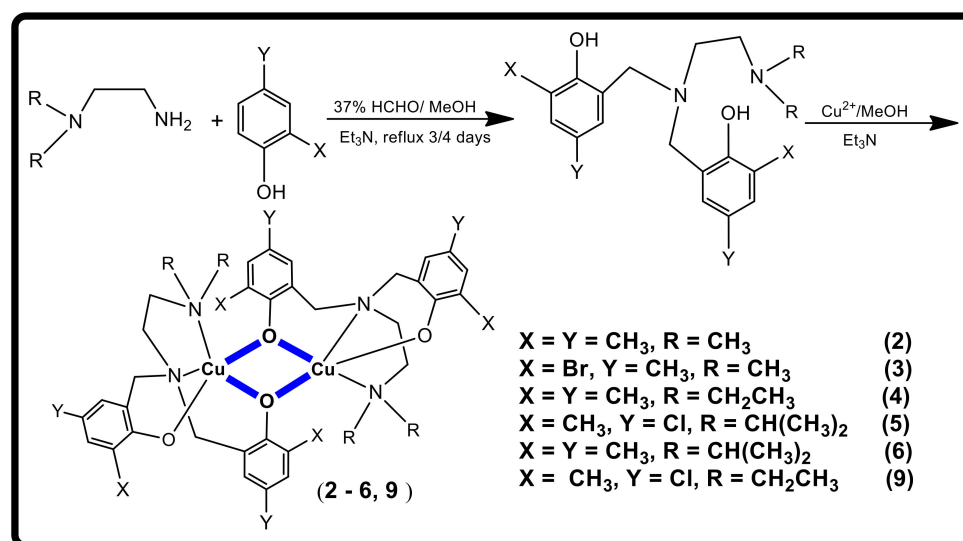
2. Results and Discussion

2.1. Synthesis of the Ligands and Complexes

The new tetradentate tripodal-phenolate amines (H_2L^1 , H_2L^4 and H_2L^9) used in this work, together with related ligands (Scheme 1), were synthesized by a standard general procedure. In a typical experiment, a methanolic mixture containing 2,4-disubstituted phenol and the corresponding amine (2:1), as well as two molar amounts of an aqueous 37% HCHO and triethylamine (Et_3N) are used, whereas in the case of 2-methoxy-phenols and pyridyl derivatives (HL^7 and HL^8 ligands, Scheme 1), equimolar ratios were employed for

all reagents. Refluxing the solutions for 3 to 4 days, followed by evaporation of the solution resulted in the formation of the solid products in reasonable yields, but about 30% were observed in the bromo-phenolate H_2L^3 . We should mention that too much evaporation of the resulting solutions may lead to the formation of an oily product and/or a semi-solid, which is hard to recrystallize and leads to impure products. The pure desired products were obtained upon recrystallization from ethyl acetate and activated charcoal (see Experimental section). The synthesis and characterization of H_2L^2 , H_2L^3 , H_2L^5 , H_2L^6 , HL^7 , HL^8 , and H_2L^{10} were recently reported by our group [30].

The doubly-bridged phenoxido Cu(II) complexes **1–6**, **9**, and the polymeric 1D **10** were obtained by the reaction of a methanolic solution of $\text{Cu}(\text{NO}_3)_2 \cdot 3\text{H}_2\text{O}$ with the corresponding tripodal-phenolate amine ligand and Et_3N in the stoichiometric 1:1:2 molar ratio. In the cationic complexes **7** and **8**, copper(II) perchlorate was used with the bipyridyl-phenolates HL^7 and HL^8 , and Et_3N (1:1:1), respectively. These reactions afforded the desired complexes in moderate to good yields (55–90%). An illustration for the synthesis of the doubly-bridged phenoxido moieties in the complexes derived from *N,N*-dialkylethylenediamines is shown in Scheme 2. Interestingly, although all double bridged phenoxido compounds display green or olive-green color, brownish-green and purple colored complexes were obtained in case of the trimeric complex **9** and the 1D-polymeric **10**. Single crystals suitable for X-ray structural determination were obtained either from dilute methanolic solution and/or recrystallization from CH_3CN or acetone. The complexes are slightly soluble in MeOH, but are more soluble in less polar solvents, such as CH_3CN and DMSO. The isolated compounds were characterized by elemental microanalyses, spectroscopic techniques, and conductivity measurements as well as by single X-ray crystallography for the copper complexes.



Scheme 2. Synthesis of the tripodal phenolate amine ligands and the doubly-bridged phenoxido-Cu(II) coordination core of complexes derived from *N,N*-dialkylethylenediamine backbone.

2.2. Characterization of the Ligands

Some very general features exist in the IR spectra of the tetradentate tripodal phenolate amine ligands, such as a very weak broad band or a shoulder over the frequency region $3140\text{--}3230\text{ cm}^{-1}$, which was attributed to the stretching vibration, $\nu(\text{O-H})$ of the phenolic groups, in addition to a series of weak to very weak bands observed over the range $2700\text{--}3050\text{ cm}^{-1}$ due to $\nu(\text{C-H})$ stretching of the aliphatic and aromatic groups. The moderate intense band detected around the $1590\text{--}1600\text{ cm}^{-1}$ region is assigned to $\nu(\text{C=N})$, whereas the moderate to strong series of bands shown in $1200\text{--}1590\text{ cm}^{-1}$ are most likely attributed to $\nu(\text{C=C}, \text{C-O})$. The ESI-MS of the ligands in MeOH, showed the 100% m/z base peak that corresponds to the protonation of parent ligand $(\text{H}_2\text{L}^n + \text{H})^+$ ($n = 2\text{--}5, 9, 10$). The ^1H NMR (d_6 -DMSO) spectra displayed peak positions at 7.1–6.8 (protons-ph);

5.0–4.9 (phenolate-protons), 3.8–3.7 (CH₂-py); 3.5–3.3 (CH₂-ph); 2.5–2.1 ppm (CH₃-ph). The pyridyl protons reveal their signals at $\delta = 8.7$ –7.1 in compounds **H₂L¹**, **HL⁴** and **HL⁸**. The hydroxyl phenolate protons were clearly observed in **H₂L¹** and **H₂L⁵** compounds but was not seen in most compounds, most likely due to their low solubility in DMSO.

2.3. Characterization of the Complexes

The IR spectra of the complexes under investigation were almost similar to the spectral pattern observed in their parent ligands, except for the disappearance of the broad band or shoulder in the region 3140–3230 cm⁻¹ of the $\nu(\text{O-H})$ of the phenolic groups upon its deprotonation and/or coordination to the Cu²⁺ ion. The two cationic perchlorate complexes **7** and **8** displayed a very strong band at 1079 and 1076 cm⁻¹, respectively, due to $\nu_{\text{as}}(\text{O-Cl})$ of the perchlorate counter ions. The O-H stretching frequency, $\nu(\text{O-H})$, for the water of crystallization in **5** and **6** and were shown as a broad band over the 3320–3400 cm⁻¹ region. The ESI-MS (CH₃CN) of the cationic pyridyl complexes **7** and **8** revealed the monomeric species with $m/z = [\text{Cu}(\text{L}^{7,8})]^+$ (100%), where the base peak (100%) of the remaining complexes was consistent with the release of the parent protonated ligands with $m/z = [\text{H}_2\text{L}^{2-6,9,10} + \text{H}]^+$.

The UV-vis spectra of the complexes under investigation, measured in DMSO and/or CH₃CN at room temperature, displayed a single broad/shoulder band in the 610–750 nm region and a strong absorption band over wavelength region 410–500 nm. The latter intense band can be assigned to the bridged phenoxido charge transfer transition (L-O → Cu^{II} LMCT) [12,20,63,64], whereas the former low intense broad band is attributed to d-d transition in five-coordinate Cu(II) complexes, which was occasionally accompanied with a weaker intense broad band around 850–890 nm. The d-d transition feature in solution is consistent with a distorted square pyramidal geometry (SP) around the central Cu(II) ion [32,48,49]. Thus, the distorted SP geometrical assignments observed in DMSO, CH₃CN, or acetone solution, were retained in the solid state (see X-ray section). The solution spectra of the complexes in these media did not show any appreciable change over the one-week period, reflecting their high stability.

The position of λ_{max} in the 610–750 nm region can be used as a criterion for the ligand field strength of the tripodal phenolate ligands; λ_{max} decreases in the order: **9** ($\lambda_{\text{max}} = 748$ nm) > **2** ($\lambda_{\text{max}} = 733$ nm) > **5** ($\lambda_{\text{max}} = 708$ nm) > **10** ($\lambda_{\text{max}} = 687$ nm) > **6** ($\lambda_{\text{max}} = 655$ nm) > **4** ($\lambda_{\text{max}} = 630$ nm) > **7** ($\lambda_{\text{max}} = 625$ nm) > **1** ($\lambda_{\text{max}} = 620$ nm). This means that the ligand field strength is decreasing in the reverse order and the strongest fields are for phenolate compounds containing pyridyl arms. However, we should mention that broadening and close location of this band in some complexes did not permit precise prediction of their actual ligand field strength, but results are consistent with previous results [65,66]. In general, ligand field strengths decrease with increasing chelate ring size, the presence of electronegative chlorine or bromine atoms in the phenolate groups, and/or steric effect on the coordinated N-aliphatic amine arms, which tends to reduce the electron density on the coordinated centers and hence its ligand field [65,66].

The non-electronic nature of all complexes, with the exception of **7** and **8**, was supported by measuring the molar conductivities, Λ_{M} in CH₃CN or DMSO, whenever the solubility permits. The measured Λ_{M} values were $\leq 5 \Omega^{-1} \cdot \text{cm}^2 \cdot \text{mol}^{-1}$, which were fully consistent with their non-ionic properties as predicted by their molecular formulas. The measured Λ_{M} values (DMSO) of the perchlorate complexes **7** and **8** were within the range of $280 \pm 2 \Omega^{-1} \cdot \text{cm}^2 \cdot \text{mol}^{-1}$. These values are in full agreement with the 1:2 electrolytic behavior of the doubly-bridged phenoxido compounds ($[\text{Cu}_2(\mu_2\text{-L}^{7,8})_2](\text{ClO}_4)_2$ (**7**, **8**) [30,67].

2.4. Description of the Structures of Complexes

The crystal structure of title compounds **3** and **4** consist of neutral dinuclear $[\text{Cu}_2(\text{L}^3)_2]$ and $[\text{Cu}_2(\text{L}^4)_2]$ units, respectively; the latter co-crystallizes with an acetone solvent molecule per dinuclear unit (Figure 1,b). In both structures, the phenolate oxygen atoms O2 and O4 of two tripod ligand **L³** or **L⁴** anions are bridging the two copper metal centers to form

four-membered Cu_2O_2 rings [Cu-O from 1.9465(16) to 2.0349(16) Å, Cu1 Cu2 = 3.047(2) (3) and 2.9949(4) Å (4); Cu1-O-Cu2 from 97.17(7) to 100.4(4)°, O-Cu-O from 74.8(4) to 75.78(7)°] (Table 1). Each Cu1 center is penta-coordinated with further three terminal sites occupied by the amine N1 and N2 atoms as well as the phenolate O1 atom. Each Cu2 center is also penta-coordinated with amine N3, N4, and phenolate O3 atoms. While the CuN_2O_3 chromophore of Cu1 may be described as less distorted square pyramid (SP) with a τ_5 -value of 0.06; the CuN_2O_3 chromophore of Cu2 is strongly distorted SP with τ_5 -value of 0.21 (3) and 0.45 (4) ($\tau = 0$ for ideal SP) and $\tau_5 = 1$ for ideal trigonal bipyramid (TBP)) [68]. Their apical positions are occupied by N2 and N4 atoms [Cu-N(apical) from 2.180(10) to 2.449(2) Å]. The Cu-N1/N3(basal) bonds vary from 2.0627(19) to 2.160(10) Å, and the Cu-O1/O3(basal) bonds from 1.8783(17) to 1.905(8) Å. The trans-basal bond angles vary from 138.62(7) to 165.55(7)°.

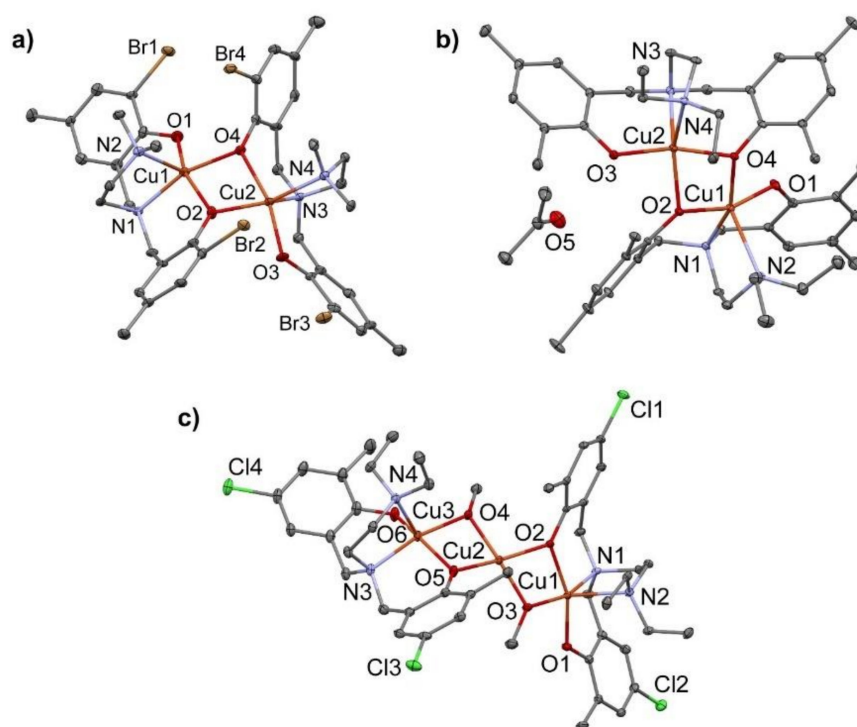


Figure 1. Perspective views of (a) 3, (b) 4, and (c) trinuclear subunit of 9.

Table 1. Selected bond distances (Å) and angles (°) of 3, 4, and 9.

3			
Cu1-N1	2.089(10)	Cu2-N3	2.160(10)
Cu1-N2	2.325(10)	Cu2-N4	2.180(10)
Cu1-O1	1.892(8)	Cu2-O3	1.905(8)
Cu1-O2	1.963(9)	Cu2-O2	2.002(8)
Cu1-O4	2.013(8)	Cu2-O4	1.999(8)
Cu1-O2-Cu2	100.4(4)	O2-Cu1-O4	75.4(3)
Cu1-O4-Cu2	98.8(4)	O2-Cu2-O4	74.8(4)
O1-Cu1-O2	157.0(4)	O3-Cu2-O4	164.3(4)
O4-Cu1-N1	160.4(4)	O2-Cu2-N4	142.0(4)

Table 1. Cont.

4			
Cu1-N1	2.0627(19)	Cu2-N3	2.090(2)
Cu1-N2	2.449(2)	Cu2-N4	2.3532(19)
Cu1-O1	1.8783(17)	Cu2-O3	1.8805(17)
Cu1-O2	1.9580(17)	Cu2-O2	2.0349(16)
Cu1-O4	2.0218(16)	Cu2-O4	1.9465(16)
Cu1-O2-Cu2	97.17(7)	O2-Cu1-O4	75.78(7)
Cu1-O4-Cu2	97.98(7)	O2-Cu2-O4	75.73(7)
O1-Cu1-O2	160.59(7)	O3-Cu2-O4	165.55(7)
O4-Cu1-N1	156.88(7)	O2-Cu2-N4	138.62(7)
9			
Cu1-N1	2.054(2)	Cu3-N3	2.066(2)
Cu1-N2	2.351(2)	Cu3-N4	2.324(2)
Cu1-O1	1.929(2)	Cu3-O4	1.941(2)
Cu1-O2	2.000(2)	Cu3-O5	1.985(2)
Cu1-O3	1.957(2)	Cu3-O6	1.944(2)
Cu2-O2	1.9488(19)	Cu2-O3	1.999(2)
Cu2-O4	1.920(2)	Cu2-O5	1.959(2)
Cu1-O2-Cu2	97.33(9)	O2-Cu1-O3	75.43(8)
Cu1-O3-Cu2	100.19(9)	O2-Cu2-O3	77.73(8)
Cu2-O4-Cu3	99.27(9)	O4-Cu2-O5	77.91(8)
Cu2-O5-Cu3	96.48(9)	O4-Cu3-O5	76.79(8)
O2-Cu2-O4	102.80(8)	O3-Cu2-O5	103.85(9)
O1-Cu1-O2	161.11(8)	O5-Cu3-O6	153.32(9)
O3-Cu1-N1	161.70(8)	O4-Cu3-N3	167.39(9)

The non-planar Cu₂O₂ four-membered rings have hinge distortion expressed by their Cu-O-Cu-O dihedral angles of 24.3° and 26.9° for **3** and **4**, respectively. The phenoxido groups deviate from phenyl out-of-plane angles (τ) of 10.5 and 12.2° in **3**, and of 3.2 and 12.8° in **4**, and phenyl ring torsion angles Cu-O-C-C of 50.9 and 71.0° in **3** and 52.5 and 67.5° in **4**.

The crystal structure of **9** features trinuclear complex units (Figure 1c) and partially disordered MeOH solvent molecules. The phenolato O2 and O5 atoms of two tripod ligand L⁹ anions and O3 and O4 of two MeO[−] anions are bridging the central Cu2 center with the two external Cu1 and Cu3 centers to form two four-membered Cu₂O₂ rings [Cu-O from 1.920(2) to 2.000(2) Å, Cu1...Cu2 = 2.9652(5), Cu2...Cu3 = 2.9418(5) Å; Cu1...Cu2...Cu3 = 154.63(2)°; Cu-O-Cu from 96.48(9) to 100.19(9)°, O-Cu-O from 75.43(8) to 77.91(8)°] (Table 1). The four oxygen atoms around Cu2 center form a tetragonally distorted square planar CuO₄ geometry with a τ_4 -value of 0.17 ($\tau_4 = 0$ for ideal square planar (SQP) and $\tau_4 = 1$ for ideal tetrahedral, (*T_d*) geometry) [9]. Coordination number 5 around the Cu1 and Cu3 center is completed by two N and one O donor atoms of two tripod L⁹ anions. Their CuN₂O₃ chromophores form SP geometry with τ_5 (Cu1) of 0.01 and τ_5 (Cu3) of 0.23. Their apical positions are occupied by N2 and N4 atoms [Cu1-N2 = 2.351(2), Cu3-N4 = 2.324(2) Å]. The Cu-N1/N3(basal) bonds are 2.054(2) and 2.066(2) Å, and the Cu-O1/O3(basal) bonds are 1.929(2) and 1.944(2) Å. The trans-basal bond angles vary from 153.32(9) to 167.39(9)°. The non-planar Cu₂O₂ four-membered rings have hinge distortion

expressed by their Cu-O-Cu-O dihedral angles of 22.9° and 23.5° . The phenoxido groups deviate from phenyl out-of-plane angles, τ of 8.2 and 20.0° , and phenyl ring torsion angles Cu-O-C-C of 44.2 and 41.9° . The trinuclear subunit may formally be created by the insertion of a “Cu(MeO)₂” moiety in the center of a bis(phenolato)-bridged Cu₂O₂ four-membered ring of a dinuclear compound (e.g., of 3).

Perspective views of the dinuclear complexes 1, 2, 5–8 containing the Cu₂O₂ bis(phenolato)-bridged subunits, as well as a section of the polymeric chain of 10, are presented in Figure 2. The crystal structures have been reported previously, along with their anticancer properties [30].

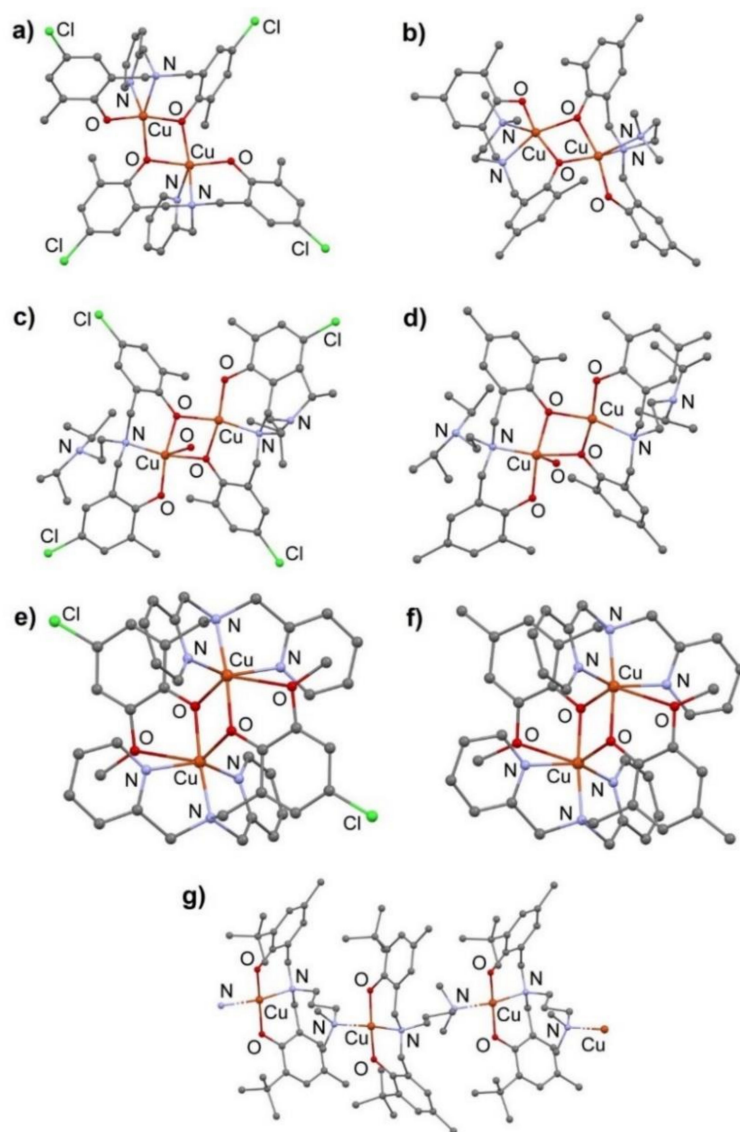


Figure 2. Perspective views of 1, 2, 5–8, and 10 represented as (a–g), respectively.

2.5. Magnetic Properties

According to the crystal structures, the complexes under investigations can be divided into six groups as follows:

Group 1: Centrosymmetric di- μ -phenoxido-bridged dinuclear complexes with a distorted square-pyramidal geometries (1 and 2). Complex [Cu₂(L¹)₂] (1) shows a distorted square-pyramidal arrangement (SP) ($\tau_5 = 0.23$) around each copper(II) center with an axial Cu-N distance of $2.310(3)$ Å, Cu···Cu distance and Cu-O-Cu angle are $3.0915(7)$ Å and $103.44(9)^\circ$, respectively [30]. Thus, Complex 1 is expected to exhibit antiferromagnetic interaction (AF) between the two $S = \frac{1}{2}$ spins through the two phenoxido bridges. Tem-

perature dependence of magnetic susceptibilities, measured under an external magnetic field of 0.5 T, ranging from 2 K to 300 K are represented in Figure 3 in the form of χ_M and μ_M vs T plots, where χ_M is the magnetic susceptibility per Cu_2 unit, μ_M is the magnetic moment per Cu_2 unit, and T is the absolute temperature. The magnetic moment of 1.30 BM at 300 K is considerably lower than the spin-only value (2.45 BM) for two non-interacting copper(II) $S = \frac{1}{2}$ ions. The magnetic moment exhibits a continuous decrease with lowering the temperature over the range 2–300 K and reaches 0.28 BM at 2 K. This magnetic behavior reveals significant AF interaction between the copper(II) ions. The magnetic data were analyzed by the Bleaney–Bowers equation based on the Heisenberg model:

$$\chi_M = (1 - p)(2Ng^2\mu_B^2/kT)[3 + \exp(-2J/kT)]^{-1} + pNg^2\mu_B^2/2kT + 2N\alpha \quad (1)$$

where g is the g value, J is the exchange coupling constant between the two copper(II) ions, p is the fraction of mononuclear copper(II) impurity, and $N\alpha$ is the temperature-independent paramagnetism for each copper(II) ion [8]. The best-fitting parameters ($g = 2.1$ (fixed), $2J = -578 \text{ cm}^{-1}$, $p = 0.016$, and $N\alpha = 60 \times 10^{-6} \text{ cm}^3 \text{ mol}^{-1}$ (fixed)) are in complete support for strong AF interaction.

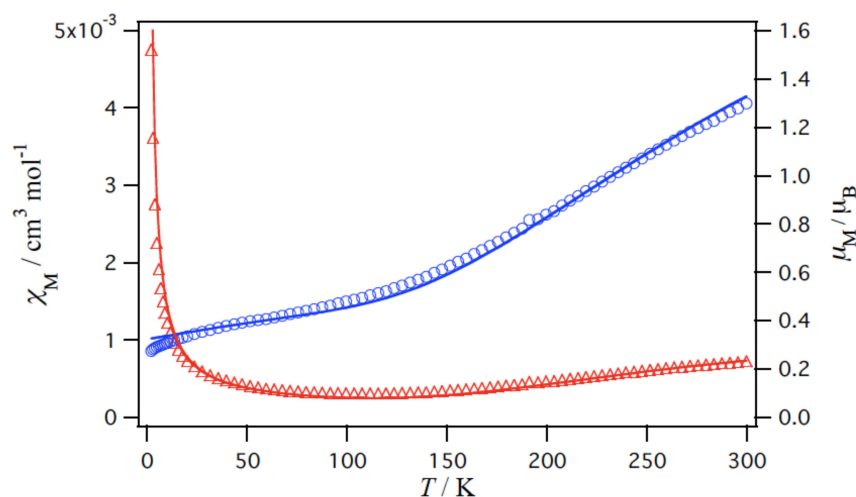


Figure 3. Temperature dependence of magnetic susceptibility χ_M (Δ) and magnetic moment μ_{eff} (\circ) of $[\text{Cu}_2(\text{L}^1)_2]$ (**1**).

The crystal structure of $[\text{Cu}_2(\text{L}^2)_2]$ (**2**) also shows the same crystallographic similarity as **1** ($\tau = 0.24$) [68] around each copper(II) center with the axial Cu–N distance of 2.3580(17) Å. The Cu···Cu distance and Cu–O–Cu angle are 3.0064(5) Å and 99.12(6)°, respectively. The μ_M of **2** is 1.62 BM per dinuclear unit at 300 K, which is also considerably lower than the spin-only value and decreases with lowering of the temperature and reaching to 0.12 BM at 2 K. The best-fitting parameters ($g = 2.10$, $2J = -403 \text{ cm}^{-1}$, $p = 0.0007$, and $N\alpha = 60 \times 10^{-6} \text{ cm}^3 \text{ mol}^{-1}$) disclose the expected strong AF interaction. The absolute $2J$ value is smaller than that of **1**, but it reflects the strong AF interaction in **1** compared **2** and is in harmony with the associated wider Cu–O–Cu angle observed in **1**.

Group 2: Pseudo-symmetric di- μ -phenoxido-bridged dinuclear complexes with distorted SP geometries (**3** and **4**). The crystal structure of $[\text{Cu}_2(\text{L}^3)_2]$ (**3**) showed that the complex exhibits distorted SP arrangements ($\tau = 0.06$ and 0.37) around two copper(II) centers with axial Cu–N distances of 2.180(10) and 2.235(10) Å. The Cu···Cu distance is 3.047(2) Å and Cu–O–Cu angles are 98.8(4) and 100.4(4)°. Complex **3** crystallizes in non-centrosymmetric with different distortion around each copper(II) center. The magnetic properties of **3** is illustrated in Figure 4. The magnetic moment of 2.07 BM at 300 K is a little higher than those of **1** and **2**, and it exhibits a gradual decrease with lowering the temperature, reaching 0.20 BM at 2 K. The magnetic data were analyzed by Equation (1), and the obtained best-fitting parameters ($g = 2.14(1)$, $2J = -291 \text{ cm}^{-1}$, $p = 0.009$, and

$N\alpha = 60 \times 10^{-6} \text{ cm}^3 \text{ mol}^{-1}$ (fixed)) demonstrates the AF interaction between the two copper(II) centers. The absolute $2J$ value of **3** is smaller than those of **1** and **2**, but with a weaker interaction. This may be attributed to the different distortion between the two copper(II) coordination environments, which causes poor overlap between the two magnetic orbitals compared to **1** and **2**.

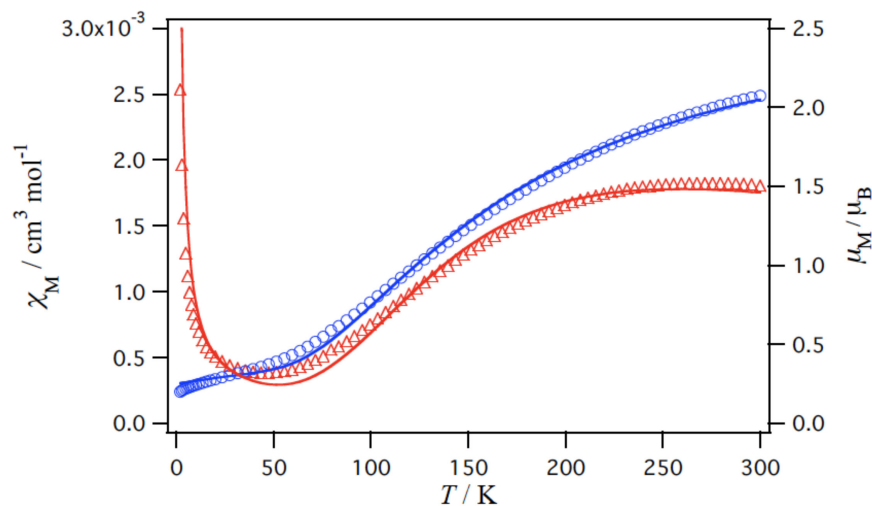


Figure 4. Temperature dependence of magnetic susceptibility χ_M (Δ) and magnetic moment μ_{eff} (\circ) of $[\text{Cu}_2(\text{L}^3)_2]$ (**3**).

The complex $[\text{Cu}_2(\mu_2\text{-L}^2)_2]$ (**4**) exhibits crystallographic similarities comparable to **3**. The molecule is a non-centrosymmetric di- μ -phenoxido-bridged complex with distorted SP arrangements ($\tau_5 = 0.07$ and 0.45) around the central copper(II) centers with the axial Cu-N distances of $2.449(2)$ and $2.3532(19)$ Å. The Cu...Cu distance and Cu-O-Cu angles are $2.9949(4)$ Å and $97.17(7)$ and $97.78(7)^\circ$, respectively. The magnetic moment μ_M (1.98 BM at 300 K) shows a gradual decrease with lowering the temperature, reaching 0.20 BM at 2 K. The magnetic data were analyzed by Equation (1) and the obtained best-fitting parameters ($g = 2.10$ (fixed), $2J = -293 \text{ cm}^{-1}$, $p = 0.008$, and $N\alpha = 60 \times 10^{-6} \text{ cm}^3 \text{ mol}^{-1}$ (fixed)) showed a comparable AF interaction to that observed in **3**. This is in accordance with the relationship between the $2J$ and Cu-O-Cu values.

Group 3: Unsymmetric di- μ -phenoxido-bridged dinuclear complexes with distorted square-pyramidal (SP) and square-planar (SQP) geometries (**5** and **6**). The crystal structure of complex $[\text{Cu}_2(\text{L}^5)_2(\text{H}_2\text{O})] \cdot 2\text{H}_2\text{O}$ (**5**) showed that the molecule exhibits a distorted SP copper(II) ($\tau_5 = 0.011$) with an axial Cu-O bond of $2.538(3)$ Å, and a distorted SQP copper(II) with the τ_4 value of 0.17. Thus, if we consider the long axial distance of $2.538(3)$ Å, then both of the magnetic orbitals of the two copper(II) centers are expected to exist within the basal NO_3 and NO_3 square plane, favoring a strong magnetic interaction. The Cu...Cu distance and Cu-O-Cu angles are 2.9331 Å, and $96.70(9)$ and $97.58(9)^\circ$, respectively. The magnetic moment, μ_M (1.82 BM at 300 K), is lower than the spin-only value (2.45 BM) for two non-interacting copper(II) $S = \frac{1}{2}$ ions. The magnetic moment revealed a gradual decrease with lowering the temperature and reaches 0.31 BM at 2 K (Figure 5). The best-fitting parameters to Equation (1) ($g = 2.1$ (fixed), $2J = -352 \text{ cm}^{-1}$, $p = 0.036$, and $N\alpha = 60 \times 10^{-6} \text{ cm}^3 \text{ mol}^{-1}$ (fixed)) are consistent with considerable AF interaction between the two copper(II) ions. The absolute $2J$ value is comparable to those obtained in **3** and **4**.

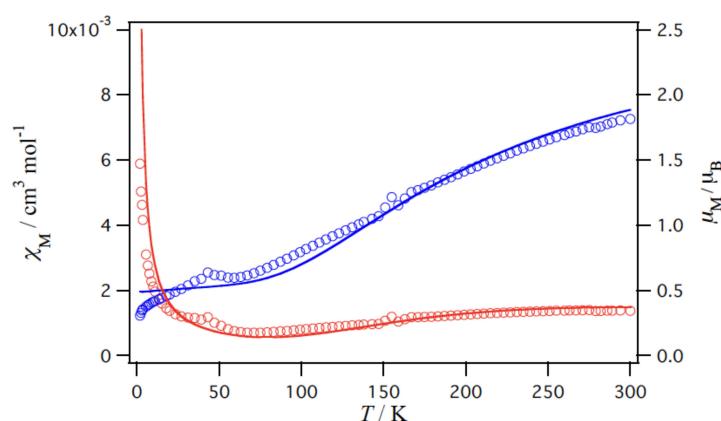


Figure 5. Temperature dependence of magnetic susceptibility χ_M (o) and magnetic moment μ_{eff} (o) of $[\text{Cu}_2(\text{L}^5)_2(\text{H}_2\text{O})]\cdot 2\text{H}_2\text{O}$ (5).

The crystal structure of $[\text{Cu}_2(\text{L}^6)_2(\text{H}_2\text{O})]\cdot 2\text{H}_2\text{O}$ (6) shows crystallographic parameters similar to 5, having a distorted SP copper(II) ($\tau_5 = 0.013$) with the axial Cu-O bond of 2.512(2) Å and a distorted SP copper(II) with τ_4 value of 0.17. The Cu...Cu distance and Cu-O-Cu angles are 2.9410(4) Å and 97.56(7) and 96.93(7)°, respectively. The magnitude of the magnetic moment of 6 is 1.68 BM at 300 K. This value is lower than the spin-only value for copper(II), $S = \frac{1}{2}$ ion, and the magnetic moment exhibits a continuous decrease with lowering temperature and reaches 0.11 BM at 2 K. The best-fitting parameters to Equation (1) ($g = 2.10$ (fixed), $2J = -500 \text{ cm}^{-1}$, $p = 0.0009$, and $N_a = 170 \times 10^{-6} \text{ cm}^3 \text{ mol}^{-1}$) showed a significant AF interaction between the two copper(II) ions. The magnetic behavior of 6 should be considered as similar to that of 5, irrespective of the relatively large $-J$ value of 5, taking into consideration the similarity of the Cu-O-Cu angle, Cu-O-Cu-O dihedral angle, phenyl ring torsion angle (Cu-O-C-C angle), and phenyl out-of-plane shift angle t (Table 2), then one should expect strong AF interaction between the copper(II) centers in the two compounds 5 and 6.

Table 2. Magnetostructural correlation of Cu_2O_2 -phenoxido complexes.

Complex	J (cm^{-1})	C.N. (Geom., τ_5 or τ_4)	Cu ... Cu (Å)	Cu-O-Cu' (°)	Cu-O-Cu-O (°)	Cu-O-C-C (°)	τ (°)
1	−289	5 (SP, 0.23)	3.092	103.44	15.9	52.1	7.8
2	−202	5 (SP, 0.24)	3.006	99.12	24.9	57.3	3.6
3	−145	5 (SP, 0.06/0.37)	3.047	98.8, 100.4	24.8	50.9, 71.0	10.5, 12.2
4	−146	5(SP, 0.07/0.45)	2.995	97.17, 97.78	26.9	52.5, 67.5	3.2, 12.8
5	−176	4(SQP, 0.17) 5(SP, 0.011)	2.9331	96.70, 97.58	29.4	50.5, 49.9	2.7, 5.5
6	−250	4(SQP, 0.17) 5(SP, 0.013)	2.941	97.56, 96.93	29.8	49.9, 51.7	6.5, 4.6
7	−3.6	5(SP, 0.41) + 1	3.130	97.72	0	11.3	31.3
8	−4.6	5(SP, 0.40) + 1	3.098	96.63	0	11.3	30.9
9	−59	4(SQP, 0.17) 5(SP: 0.01, 0.23)	2.9652 2.9418	96.48, 97.33, 99.27, 100.19	22.9, 23.5	44.2, 41.9	8.2, 20.0
10	+3.5	4(SQP, 0.23)	7.269				

Group 4: Centrosymmetric di(phenoxido)-bridged dinuclear complexes with a distorted (5 + 1) octahedral geometries (7 and 8). The crystal structural analysis of $[\text{Cu}_2(\text{L}^7)_2](\text{ClO}_4)_2$ (7) shows a distorted octahedral (5 + 1) geometry with a semi-coordination Cu-OMe of

2.785(4) Å around each copper(II) center. If this semi-coordination is neglected as a substantial bond because of its long distance, then the coordination geometry can be regarded as a distorted square-pyramidal geometry with the τ_5 value of 0.41. Therefore, taking into consideration the long distance of the axial Cu-O(phenoxido) bond of 2.213(3) Å, as a result the magnetic orbital of each copper(II) ion may exist around the basal N₃O plane mainly and not in the direction of the axial phenoxido-bridging bond, which leads to a poor magnetic interaction. The Cu⋯Cu distance and Cu-O-Cu angle are 3.130 Å and 97.72 (14)°, respectively. The magnetic data of **7** are illustrated in Figure 6. The μ_B (2.65 BM at 300 K) is higher than the spin-only value (2.45 BM) for two non-interacting copper(II), $S = \frac{1}{2}$ ions. The magnetic moment exhibits a continuous decrease with lowering temperature and reaches 0.51 BM at 2 K, suggesting an AF interaction. The best-fitting parameters ($g = 2.14$, $2J = -7.2 \text{ cm}^{-1}$, and $N\alpha = 60 \times 10^{-6} \text{ cm}^3 \text{ mol}^{-1}$ (fixed)) are consistent with a weak AF interaction between the two copper(II) ions.

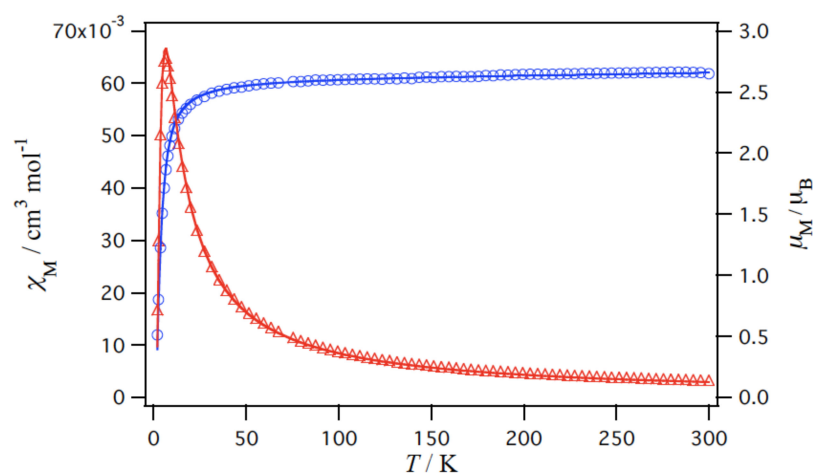


Figure 6. Temperature dependence of magnetic susceptibility χ_M (Δ) and magnetic moment μ_{eff} (\circ) of $[\text{Cu}_2(\text{L}^7)_2](\text{ClO}_4)_2$ (**7**).

Complex $[\text{Cu}_2(\text{L}^8)_2](\text{ClO}_4)_2$ (**8**) exhibits very close crystallographic parameters like **7**; distorted octahedral (5 + 1) arrangement with a semi-coordination of Cu-OMe of 2.791(3) Å around each copper(II) ion. The coordination geometry of this complex is similar to **7** and can be regarded as indicated above as a distorted SP geometry (τ_5 value of 0.40) with a relatively long axial phenoxido-bridging of Cu-O distance of 2.215(2) Å. The Cu⋯Cu distance and the Cu-O-Cu angle are 3.098(2) Å and 96.63(10)°, respectively. The similarity was also extended to the magnetic properties of **7**. The best-fitting parameters ($g = 2.1$ (fixed), $2J = -9.2 \text{ cm}^{-1}$, and $N\alpha = 60 \times 10^{-6} \text{ cm}^3 \text{ mol}^{-1}$ (fixed)) shows a weak AF interaction between the two copper(II) ions.

In **7** and **8**, the Cu_2O_2 bridging ring with the axial phenoxido-bridges is planar, as can be seen from the Cu-O-Cu-O dihedral angle of 0° (Table 2), and thus the magnetic orbitals of each copper(II) ion should be parallel to each other. This suggests that the phenoxido oxygens are rather axially located relative to the basal dx^2-y^2 orbital plane. Such axial bridging oxygens cannot effectively participate in mediating the magnetic interaction through the phenoxido-bridges.

Group 5: linear trinuclear complex **9**. The crystal structure of $[\text{Cu}_3(\text{L}^9)_2(\mu\text{-OCH}_3)_2]\cdot\text{CH}_3\text{COCH}_3$ (**9**) shows that the molecule has a μ -phenoxido- μ -methoxido-bridged trinuclear copper(II) complex with a linear arrangement of the three copper(II) ions. The magnetic data (Figure 7) revealed a magnetic moment of 2.50 BM at 300 K, which is lower than the spin-only value (3.00 BM) for three non-interacting copper(II), $S = \frac{1}{2}$ ions. The magnetic moment exhibits a gradual decrease with lowering temperature and reaches 1.46 BM at 2 K. This behavior suggests a remarkable AF interaction between the copper(II) ions. The magnetic analysis was carried out with the susceptibility equation for the linear trinuclear copper(II) ions based on $\mathcal{H} = -2J_{\text{Cu}_3}(S_1 \cdot S_2 + S_2 \cdot S_3)$. However, the

fitting was not good, and rather better fitting was obtained when the magnetic data were analyzed by the dinuclear model using Equation (1). The results indicated that the magnetic data of **9** contain some impurities arising from the presence of dinuclear copper(II) species. Therefore, the magnetic data were analyzed with the aid of Equation (2) of linear trinuclear and dinuclear copper(II) model.

$$\chi_M = (1 - p_{Cu2})(Ng^2\mu_B^2/4kT)[1 + \exp(-2J_{Cu3}/kT) + 10\exp(J_{Cu3}/kT)]/[1 + \exp(-2J_{Cu3}/kT) + 2\exp(J_{Cu3}/kT)] + p_{Cu2}(2Ng^2\mu_B^2/kT)[3 + \exp(-2J/kT)]^{-1} + (3 - p_{Cu2})N\alpha \quad (2)$$

where p_{Cu2} is the fraction of dinuclear copper(II) impurity. The best-fitting parameters ($g = 2.1$ (fixed), $J_{Cu3} = -59 \text{ cm}^{-1}$, $p_{Cu2} = 0.315$, $2J = -592 \text{ cm}^{-1}$, and $N\alpha = 60 \times 10^{-6} \text{ cm}^3 \text{ mol}^{-1}$ (fixed)) revealed the existence of a considerable amount of dinuclear copper(II) species in the sample.

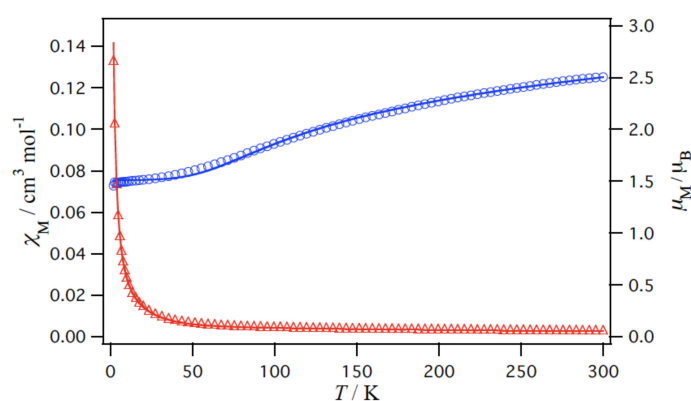


Figure 7. Temperature dependence of magnetic susceptibility χ_M (Δ) and magnetic moment μ_{eff} (\circ) of $[\text{Cu}_3(\text{L}^9)_2(\mu\text{-OCH}_3)_2]$ (**9**).

Group 6: polynuclear chain complex **10**. The X-ray structure analysis revealed that catena- $[\text{Cu}(\mu\text{-L}^{10})]$ (**10**) is a polynuclear chain molecule constructed of tetrahedrally distorted square-planar $[\text{Cu}(\text{L}^{10})]$ units ($\tau_4 = 0.23$) [9] with $\text{Cu}\cdots\text{Cu}$ distance of 7.269 Å. The temperature dependence of magnetic susceptibilities χ_A and magnetic moments μ_A are represented in Figure 8, where χ_A and μ_A are per Cu unit. The μ_A value of 1.83 BM at 300 K is a little bit higher than the spin-only value (1.73 BM) for copper(II), $S = \frac{1}{2}$ ion. The μ_A vs. T plot shows a slight gradual increase with a lowering of the temperature over the range 50–300 K and a gradual decrease on lowering the temperature from 50 to 2 K, reaching, 1.70 BM at 2 K. While the increase of the μ_A value suggests F interaction between two adjacent Cu(II) centers via the L^{10} anion ligand, the corresponding decrease in μ_A values indicates an AF intermolecular interaction. The magnetic data were analyzed by the molecular field approximation (Equation (3) [8]), where for this series Equation (4) for the Heisenberg model for ferromagnetically coupled $S = \frac{1}{2}$ ions (derived by Baker et al. [10]), considering the magnetic interaction between the neighboring chain molecules as zJ' (z = number of interacting neighbors), was used:

$$\chi_A' = \chi_A / \{1 - (2zJ' / Ng^2\mu_B^2)\chi_A\} \quad (3)$$

$$\chi_A = (Ng^2\mu_B^2/4kT)[(1.0 + 5.7979916x + 16.902653x^2 + 29.376885x^3 + 29.832959x^4 + 14.036918x^5)/(1.0 + 2.7979916x + 7.0086780x^2 + 8.6538644x^3 + 4.5743114x^4)]^{2/3} + N\alpha \quad (4)$$

where $x = J/2kT$. The solid line in Figure 8 shows the calculated curve with best-fitting parameters of $g = 2.1$ (fixed), $J = 3.5 \text{ cm}^{-1}$, $N\alpha = 60 \times 10^{-6} \text{ cm}^3 \text{ mol}^{-1}$ (fixed), and $zJ' = -2.9 \text{ cm}^{-1}$.

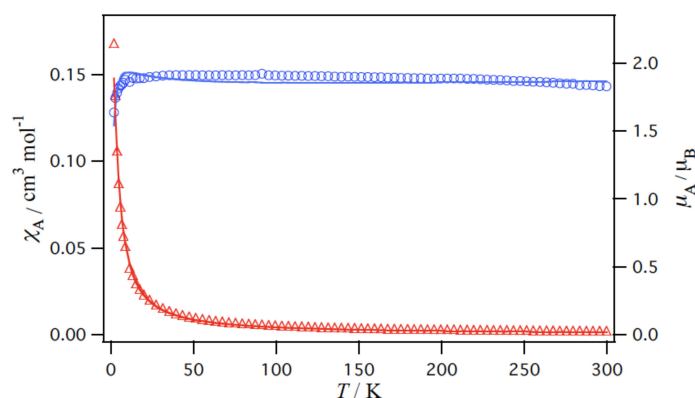


Figure 8. Temperature dependence of magnetic susceptibility χ_M (Δ) and magnetic moment μ_{eff} (\circ) of $[\text{Cu}(\text{L}^{10})]$ (**10**).

3. Conclusions

In this work eight dinuclear doubly-bridged-phenoxido copper(II) complexes revealed antiferromagnetic coupling (AF) varied from strong AF interaction ($-J = 289\text{--}145 \text{ cm}^{-1}$) for complexes **1–6** to very weak AF interaction ($-J = 3.6$ & 4.6 cm^{-1}) in **7** and **8**. The geometry around the central Cu(II) centers exhibits distorted square-pyramidal arrangement in the first four complexes, mixed square pyramidal and distorted square planar in **5** and **6**, and distorted pseudo octahedral ($5 + 1$) arrangements in **7** and **8**. Attempts were made to correlate the exchange coupling (J) to the structural parameters of the non-planar Cu_2O_2 four-membered rings. These parameters include the $\text{Cu}\cdots\text{Cu}$ distances ($2.941\text{--}3.130 \text{ \AA}$), Cu-O-Cu bond angles ($96.93\text{--}103.44^\circ$) [69,70], Cu-O-Cu-O dihedral angles ($0\text{--}29.8^\circ$), and the deviation angles of the phenoxido groups from the phenyl out-of-plane angles ($11.3\text{--}71.0^\circ$) as well as the phenyl ring torsion angles Cu-O-C-C ($2.7\text{--}31.3$). Unfortunately, no satisfied correlations were observed between J and the mentioned geometrical parameters [69,70]. This is most likely due to the influence of the steric environment incorporated by the substituents into phenolate groups, and the terminal coordinated dialkylamine, and hence the geometrical arrangement around the central Cu(II) ions as well as the coplanarity of the phenolate groups with the bridging Cu_2O_2 moiety [53,70,71]. These factors may play a key role in reducing the efficient overlap between the $3d$ Cu^{2+} and $2p$ O-phenoxido magnetic orbitals bearing the unpaired electrons. In general and focusing the discussion only on Cu(II) complexes containing mono- and doubly-bridged phenoxido compounds with no other bridging ligands, our results agree with the magnetic properties determined in many phenoxido-bridged copper complexes, where relatively strong AF couplings were reported [1,54,69,70,72], regardless of the fact that some of these compounds were ferromagnetically coupled [1,54,72,73].

In contrast and unlike the bridged bis(phenoxido) dinuclear copper(II) complexes, where no correlation was observed between J and Cu-O-Cu bond angle, linear relationships were obtained in the corresponding bis(hydroxido) [74] and bis(alkoxido) [75] bridged copper(II) complexes. In addition, a similar linear correlation was reported in bis(phenoxido) macrocyclic complexes in which the unique conjugated π -electron inherited into the macrocycle skeleton constrained the ligand to adopt a planar configuration [71]. On the other hand, a relatively moderate AF coupling ($-J = 59 \text{ cm}^{-1}$) was evaluated in the trinuclear **9**, where alternative bridged phenoxido and methoxido groups were determined. However, in the 1D polymer **10**, a weak ferromagnetic interaction ($J = +3.5 \text{ cm}^{-1}$) was obtained. Interestingly, in the latter complex, the Cu(II) centers were linked via the *N,N*-dimethylpropyl arms with long $\text{Cu}\cdots\text{Cu}$ distance (7.269 \AA) and a tetrahedral distorted square planar four-coordinate geometry around each Cu(II) center [30].

4. Experimental

4.1. Materials and Physical Measurements

N,N-Dimethyl-, *N,N*-diethyl-, *N,N*-isopropyl-ethylenediamine, 3-dimethylamino-propylamine, 2,4-dimethylphenol, 4-chloro-2-methylphenol, 2-bromo-4-methylphenol, 2-methoxy-4-methylphenol, 4-chloro-2-methoxyphenol and 2-*tert*-butyl-4-methylphenol, picolylamine as well as dipicolylamine were purchased from TCI-America. All other chemicals were commercially available and used without further purification.

Electronic spectra were recorded using an Agilent 8453 HP diode array UV-Vis spectrophotometer. Infrared spectra were recorded on a Cary 630 (ATR-IR) spectrometer. ^1H spectra were obtained at room temperature on a Varian 400 NMR spectrometer operating at 400 MHz (^1H). ^1H NMR chemical shifts (δ) are reported in ppm and were referenced internally to residual solvent resonances (d_6 -DMSO: $\delta_{\text{H}} = 2.49$) or TMS. ESI-MS of organic compounds and their Cu(II) were measured in MeOH and CH_3CN , respectively, on a LC-MS Varian Saturn 2200 Spectrometer. Conductivity measurements were performed using a Mettler Toledo Seven Easy conductivity meter and calibrated by 1413 $\mu\text{S}/\text{cm}$ conductivity standard. The molar conductivity of the complexes was determined from $\Lambda_{\text{M}} = (1.0 \times 10^3 \kappa)/[\text{Cu(II)}]$, where κ = specific conductance and $[\text{Cu}^{\text{II}}]$ is the molar concentration of the complex. Elemental microanalyses were carried out by Atlantic Microlaboratory, Norcross, Georgia U.S.A.

The temperature dependent magnetic susceptibilities were measured over 2–300 K at the constant field of 0.5 T with a Quantum Design MPMS 3 (installed at Shimane University) for 1–3, 4, 6–10, and with a Quantum Design MPMS-7 (installed at Institute for Molecular Science (IMS)) for 5. The measured data were corrected for diamagnetic contributions [76].

4.2. Synthesis of the Organic Ligands

The new ligands H_2L^3 , H_2L^4 and H_2L^9 illustrated in Scheme 1, and their characterization are given below, whereas the rest of the ligands shown in this scheme (H_2L^1 , H_2L^2 , H_2L^5 , H_2L^6 , and H_2L^{10} as well as HL^7 and H_2L^8) were recently reported [30].

4.2.1. 6,6'-(((2-(Dimethylamino)ethyl)azanediyl)bis(methylene))bis(2-bromo-4-methylphenol) (H_2L^3)

To a mixture containing 2-bromo-4-methylphenol (3.740 g, 20 mmol), Et_3N (2.04 g, 20 mmol) and aqueous 37% HCHO (1.63 g, 20 mmol) dissolved in methanol (50 mL), *N,N*-dimethylethylenediamine (0.882 g, 10 mmol). The mixture was stirred and refluxed gently for 3 days. Evaporating the resulting solution under reduced pressure resulted in the formation of white crystalline compound, which was then filtered, washed with Et_2O , and air dried (yield: 4.35 g, 89.5%). Characterization: calcd for $\text{C}_{20}\text{H}_{26}\text{Br}_2\text{N}_2\text{O}_2$ (MM = 486.241 g/mol): C, 49.40; H, 5.39; N, 5.76%. Found: C, 49.44; H, 5.51; N, 5.78% m.p. 189° C. IR bands (ATR, cm^{-1}): 2972 (w), 2950 (vw), 2820 (w), $\nu(\text{C-H})$; 1480 (s), 1458 (vs), 1446 (s), 1374 (s), 1291 (s), 1231 (s), 1204 (s) $\nu(\text{C=C, C-N, C-O})$; 1165 (s), 1122 (s), 1047 (m), 924 (s), 902 (s), 809 (vs). ESI-MS: $m/z = 487.042$, calcd [$\text{H}_2\text{L}^6 + \text{H}$] $^+ = 487.042$.

4.2.2. 6,6'-(((2-(Diethylamino)ethyl)azanediyl)bis(methylene))bis(2,4-dimethylphenol) (H_2L^4)

This compound was synthesized using a similar procedure and the same molar ratios as that described above for H_2L^3 , except 2,4-dimethylphenol (2.44 g, 20 mmol) and *N,N*-dimethylethylenediamine (1.162 g, 10 mmol) were used instead of 2-bromo-4-methylphenol and *N,N*-dimethylethylenediamine, respectively (yield: 2.57 g, 66.8%). Characterization: m.p. 137–140° C. Anal. calcd for $\text{C}_{24}\text{H}_{36}\text{N}_2\text{O}_2$ (MM = 384.555 g/mol): C, 74.96; H, 9.44; N, 7.28%. Found: C, 74.81; H, 9.56; N, 7.28%. IR bands (ATR, cm^{-1}): 2978 (vw), 2937 (vw), 2913 (vw), 2904 (m), 2802 (w) $\nu(\text{C-H})$; 1484 (vs), 1376 (m), 1224 (vs) $\nu(\text{C=C, C-O})$; 1152 (s), 1129 (m), 1096 (m), 1024 (m), 922 (m), 864 (s), 805 (m), 743 (vs). ESI-MS: $m/z = 585.286$ (100%), calcd [$\text{H}_2\text{L}^2 + \text{H}$] $^+ = 585.285$. ^1H NMR (d_6 -DMSO, 400 MHz, δ in ppm): 6.84, 6.66 (2H, 2s, 1:1, ph); 3.55 (2H, s, CH_2 -ph); 2.59 (2H, m, N-CH_2 - CH_3); 2.40 (4H, m, N-CH_2 - CH_2 -N); 2.14,

2.07 (3H, 2s, 1:1, 2xCH₃-ph); 0.96 (3H, t, CH₃-CH₂). ¹³C NMR: 152 (HO-C₆H₄); 131.0, 128.2, 127.3, 125.39, 121.44 (C-ph); 55.8 (N-CH₂ph); 49.8, 48.7 (N-CH₂-CH₂-N); 45.7 (CH₂CH₃); 20.4 (H₃C₄ph); 16.1 (H₃C₂ph); 9.9 (CH₂CH₃).

4.2.3.

6,6'-(((2-(Diethylamino)ethyl)azanediyl)bis(methylene))bis(4-chloro-2-methylphenol) (**H₂L⁹**)

A mixture of 4-chloro-2-methylphenol (2.825 g, 20 mmol), Et₃N (2.022 g, 20 mmol), aqueous 37% HCHO (1.627 g, 20 mmol) and N,N-diethylethylenediamine (1.162 g, 10 mmol) was dissolved in methanol (60 mL). The mixture was stirred and refluxed gently for 3 days. Evaporating this solution under reduced pressure resulted in the formation of white precipitate, which was then collected by filtration, washed with Et₂O, and air dried (yield: 2.35 g, 55.3%). Characterization: m.p. 137–141 °C. Calcd for C₂₂H₃₀Cl₂N₂O₂ (MM = 424.168 g/mol): C, 62.12; H, 7.11; N, 6.59%. Found: C, 62.29; H, 7.21; N, 6.53%. IR bands (ATR, cm⁻¹): 2981 (w), 2915 (vw), 2814 (w) ν(C-H); 1583 (w), 1467 (vs), 1378 (m), 1324 (m), 1273 (s), 1226 (vs) ν(C=C, C-O); 1126 (m), 1093 (s), 1063 (m), 1023 (m), 976 (m), 929 (m), 864 (vs), 804 (m) 739 (vs), 669 (m). ESI-MS: *m/z* = 425.175 (100%), calcd [**H₂L⁴** + H]⁺ = 425.176. ¹H NMR (*d*₆-DMSO, 400 MHz, δ in ppm): 7.05, 7.00 (2H, 2s, 1:1, 2xHph); 3.58 (2H, s, CH₂-ph); 3.37 (2H, m, N-CH₂-CH₃); 2.44 (3H, t, N-CH₂-CH₂-N); 2.11 (3H, s, CH₃-ph); 0.97 (3H, t, CH₃-CH₂-).

4.3. Synthesis of Copper(II) Complexes

A general method was used to synthesize the copper(II) complexes **3**, **4**, and **9**: to a mixture containing the appropriate tripod phenolate-amine ligand (0.5 mmol) and Et₃N (0.102 g, 1.00 mmol) dissolved in MeOH (20–30 mL), Cu(NO₃)₂·3H₂O (0.122 g, 0.5 mmol) was added, and the resulting solution was heated for 5–10 min, filtered while hot through celite and allowed to crystallize at room temperature. The precipitate, which was collected by filtration, was washed with Et₂O and dried in air. Crystals suitable for X-ray analysis were obtained from dilute methanolic solutions or by recrystallization from CH₃CN, but acetone was used in complex **4**.

4.3.1. [Cu₂(μ₂-L³)₂] (**3**)

The reaction of Cu(NO₃)₂·3H₂O with H₂L³ and Et₃N (1:1:2) in MeOH, as indicated above, resulted in the formation a crude product, which upon recrystallization from CH₃CN, afforded large dark green crystalline compound (yield: 81.6%). Anal: calcd for C₄₀H₄₈Br₄Cu₂N₄O₄ (MM = 1089.90 g/mol): C, 43.85; H, 4.42; N, 5.11%. Found: C, 44.03; H, 4.47; N, 5.42%. IR bands (ATR, cm⁻¹): 2969 (vw), 2860 (vw), 2831 (vw), 2784 (vw) ν(C-H); 1603 (w), 1464 (vs), 1378 (w), 1278 (m), 1238 (s) ν(C=C, C-O, C-N); 1125 (m), 839 (s), 795 (s), 768 (s), 594 (m), 569 (m), 493 (m), 467 (m), 411 (s). ESI-MS (CH₃CN): *m/z* = 487.042. (100%), calcd [**H₂L³** + H]⁺ = 487.042. UV-VIS: λ_{max} in nm (ε_{max}, M⁻¹cm⁻¹): in DMSO: 452 (2330), 763 (216, b). Λ_M (DMSO) = 3.0 Ω⁻¹·cm²·mol⁻¹.

4.3.2. [Cu₂(μ₂-L⁴)₂]·CH₃COCH₃ (**4**)

This complex was isolated as big chunks of light olive-green solid (yield: 98 mg, 82.9%). Recrystallization from acetone afforded X-ray quality crystals. Anal: calcd for C₅₁H₇₄Cu₂N₄O₅ (MM = 948.425 g/mol): C, 64.46; H, 7.85; N, 5.90%. Found: C, 64.62; H, 7.88; N, 6.03%. IR bands (ATR, cm⁻¹): 2966 (w), 2903 (w), 2840 (w) ν(C-H); 1609 (w) ν(C=N); 1479 (s), 1377 (m), 1319 (s), 1243 (s) ν(C=C, C-O); 1158 (m), 1091 (m), 1017 (m), 972 (m), 855 (vs), 794 (s), 751 (s), 729 (m). ESI-MS (CH₃CN): 385.285 (100%), calcd [**H₂L⁴** + H]⁺ = 385.286. UV-VIS in acetone: λ_{max} in nm (saturated solution): 409, 630 (b).

4.3.3. [Cu₃(μ₂-L⁹)₂(μ-OCH₃)₂]·CH₃OH (**9**)

The complex was isolated as shiny brownish-green crystalline compound after recrystallization from acetone (yield: 69.3%). Anal: calcd for C₄₇H₆₆Cl₄Cu₃N₄O₆

(MM = 1131.500 g/mol): C, 49.89; H, 4.88; N, 4.95%. Found: C, 50.44; H, 5.16; N, 5.37%. IR bands (ATR, cm^{-1}): 2976 (w), 2922 (vw), 2845 (w) $\nu(\text{C-H})$; 1585 (w) $\nu(\text{C=N})$; 1462 (vs), 1285 (s), 1243 (vs) $\nu(\text{C=C, C-O, C-N})$; 1010 (m), 935 (w), 864 (s), 766 (vs), 747 (s), 661 (m), 449 (s). ESI-MS: $m/z = 425.176$ (100%), calcd $[\text{H}_2\text{L}^9 + \text{H}]^+ = 425.176$. UV-VIS: λ_{max} in nm ($\epsilon_{\text{max}}, \text{M}^{-1}\text{cm}^{-1}$): in DMSO: 447 (2650), 748 (251, b). Λ_{M} (DMSO) = $3.5 \Omega^{-1}\cdot\text{cm}^2\cdot\text{mol}^{-1}$.

4.4. X-ray Crystal Structure Analysis

The X-ray single-crystal data of the title compounds **3**, **4**, and **9** were collected on a Bruker-AXS APEX II CCD diffractometer at 100 (2) K. The crystallographic data, conditions retained for the intensity data collection and some features of the structure refinements are listed in Table 3. Data collections were performed with Mo-K α radiation ($\lambda = 0.71073 \text{ \AA}$); data processing, Lorentz-polarization, and absorption corrections were performed using APEX and the SADABS computer programs [77–79]. The structures were solved by direct methods and refined by full-matrix least-squares methods on F^2 , using the SHELX [80–82] program library. Additional programs used: Mercury and PLATON [83]. Packing plots are given in the Supplementary Materials (Figures S1–S3).

Table 3. Crystallographic data and processing parameters of **3**, **4**, and **9**.

Compound	3	4	9
Empirical formula	$\text{C}_{40}\text{H}_{48}\text{Br}_4\text{Cu}_2\text{N}_4\text{O}_4$	$\text{C}_{51}\text{H}_{74}\text{Cu}_2\text{N}_4\text{O}_5$	$\text{C}_{47}\text{H}_{62}\text{Cl}_4\text{Cu}_3\text{N}_4\text{O}_7$
Formula mass	1095.53	950.22	1131.45
System	Monoclinic	Triclinic	Monoclinic
Space group	$\text{P}2_1/\text{c}$	P-1	$\text{P}2_1/\text{n}$
a (\AA)	15.433(3)	12.6538(12)	10.7647(5)
b (\AA)	14.198(3)	13.0192(12)	29.4374(14)
c (\AA)	20.973(4)	15.4646(15)	16.5922(8)
α ($^\circ$)	90	95.347(5)	90
β ($^\circ$)	100.460(7)	101.633(5)	90.673(2)
γ ($^\circ$)	90	103.880(4)	90
V (\AA^3)	4519.2(16)	2395.5(4)	5275.5(4)
Z	4	2	4
θ max ($^\circ$)	26.000	30.558	24.999
Data collected	82442	133738	159804
Unique refl.	8840	14144	9251
Parameters	495	573	600
Goodness-of-fit on F^2	1.069	1.057	1.109
R1/wR2 (all data)	0.1102/0.2845	0.0528/0.1336	0.0357/0.0923

Supplementary Materials: The following are available online at <https://www.mdpi.com/article/10.3390/molecules28062648/s1>. CCDC 2241168–2241170 contains the supplementary crystallographic data for **3**, **4**, and **9**, respectively. These data can be obtained free of charge via <http://www.ccdc.cam.ac.uk/conts/retrieving.html>, or from the Cambridge Crystallographic Data Centre, 12 Union Road, Cambridge CB2 1EZ, UK; fax: (+44) 1223-336-033; or e-mail: deposit@ccdc.cam.ac.uk. Further supplementary data for Packing plots (Figures S1–S3) and Figure S4 for temperature dependence of magnetic susceptibility and magnetic moment μ_{eff} of **2**. Table S1: Crystallographic data and processing parameters of **3**, **4** and **9**.

Author Contributions: Conceptualization, Methodology, Validation, Investigation, Resources, Data curation, Writing—original draft, Writing—review & editing, Visualization, Supervision, Project

administration, Funding acquisition: S.S.M., F.A.M., M.M. and M.H.; Methodology, Validation, Formal analysis, Investigation. Writing—review & editing: F.R.L. and N.N.M.H.S.; Methodology, Software, Validation, Formal analysis, Investigation, Data curation: R.C.F. and A.T.; Methodology, Formal analysis, Investigation, Data curation, Investigation, Resources, Data curation: M.T.D. and K.N. All authors have read and agreed to the published version of the manuscript.

Funding: This research received no external funding.

Institutional Review Board Statement: Not applicable.

Informed Consent Statement: Not applicable.

Data Availability Statement: Data is contained within the available article and Supplementary Materials.

Acknowledgments: This research was financially supported by the Department of Chemistry—University of Louisiana at Lafayette. Our thanks also to the reviewers for their constructive comments and suggestions.

Conflicts of Interest: The authors declare no conflict of interest.

Sample Availability: Samples of the compounds 1–10 are not available.

References

1. Massoud, S.S.; Spell, M.; Ledet, C.; Junk, T.; Herchel, R.; Fischer, R.C.; Travnicek, Z.; Mautner, F.A. Magnetic and structural properties of dinuclear singly bridged-phenoxido metal(II) complexes. *Dalton Trans.* **2015**, *44*, 2110–2121. [[CrossRef](#)]
2. Massoud, S.S.; Junk, T.; Louka, F.R.; Herchel, R.; Travnicek, Z.; Fischer, R.C.; Mautner, F.A. Synthesis, structure and magnetic characterization of dinuclear copper(II) complexes bridged by bicompartamental phenolate. *RSC Adv.* **2015**, *5*, 87139–87150. [[CrossRef](#)]
3. Massoud, S.S.; Junk, J.; Herchel, R.; Travnicek, Z.; Mikuriya, M.; Fischer, R.C.; Mautner, F.A. Structural characterization of ferromagnetic bridged-acetato and -dichlorido copper(II) complexes based on bicompartamental 4-*t*-butylphenol. *Inorg. Chem. Commun.* **2015**, *60*, 1–3. [[CrossRef](#)]
4. Massoud, S.S.; Ledet, C.C.; Junk, T.; Bosch, S.; Comba, P.; Herchel, R.; Hošek, J.; Trávníček, Z.; Fischer, R.C.; Mautner, F.A. Dinuclear metal(II)-acetato complexes based on bicompartamental chlorophenol: Synthesis, structure, magnetic properties, DNA interaction and phosphodiester hydrolysis. *Dalton Trans.* **2016**, *45*, 12933–12950. [[CrossRef](#)] [[PubMed](#)]
5. Mikuriya, M.; Sato, S.; Yoshioka, D. μ -Phenolato- μ -acetato-bridged dinuclear copper(II) complex with dinucleating Schiff-base ligand having three phenolate groups. *X-Ray Struct. Anal. Online* **2018**, *34*, 45–47. [[CrossRef](#)]
6. Mikuriya, M.; Sato, S.; Yoshioka, D. μ -Phenolato- μ -benzoato-bridged dinuclear copper(II) cluster with a ferromagnetic coupling. *X-Ray Struct. Anal. Online* **2018**, *34*, 51–53. [[CrossRef](#)]
7. Kakuta, Y.; Masuda, N.; Kurushima, M.; Hashimoto, T.; Yoshioka, D.; Sakiyama, H.; Hiraoka, Y.; Handa, M.; Mikuriya, M. Synthesis, crystal structures, spectral, electrochemical, and magnetic properties of di- μ -phenoxido-bridged dinuclear copper(II) complexes with *N*-salicylidene-2-hydroxybenzylamine derivatives: Axial coordination effect of dimethyl sulfoxide molecule. *Chem. Pap.* **2014**, *68*, 923–931. [[CrossRef](#)]
8. Mikuriya, M.; Yamakawa, C.; Tanabe, K.; Nukita, R.; Amabe, Y.; Yoshioka, D.; Mitsuhashi, R.; Tatehata, R.; Tanaka, H.; Handa, M. Copper(II) carboxylates with 2,3,4-trimethoxybenzoate and 2,4,6-trimethoxybenzoate: Dinuclear Cu(II) cluster and μ -aqua-bridged Cu(II) chain molecule. *Magnetochemistry* **2021**, *7*, 35. [[CrossRef](#)]
9. Yang, L.; Powell, D.R.; House, R.P. Structural variation in copper(I) complexes with pyridylmethylamide ligands: Structural analysis with a new four-coordinate geometry index, τ_4 . *Dalton Trans.* **2007**, *9*, 955–964. [[CrossRef](#)]
10. Mautner, F.A.; Koikawa, M.; Mikuriya, M.; Harrelson, E.V.; Massoud, S.S. Copper(II)-azido complexes constructed from polypyridyl amine ligands. *Polyhedron* **2013**, *59*, 17–22. [[CrossRef](#)]
11. Mukherjee, J.; Mukherje, R. Catecholase activity of dinuclear copper(II) complexes with variable endogenous and exogenous bridge. *Inorg. Chim. Acta* **2002**, *337*, 429–438. [[CrossRef](#)]
12. Karlin, K.D.; Farooq, A.; Hayes, J.C.; Cohen, B.I.; Rowe, T.M.; Sinn, E.; Zubieta, J. Models for met-hemocyanin derivatives: Structural and spectroscopic comparisons of analogous phenolate and X (X = OH[−], OMe[−], N₃[−], Cl[−], OAc[−], OBz[−]) doubly bridged dinuclear copper(II) complexes. *Inorg. Chem.* **1987**, *26*, 1271–1280. [[CrossRef](#)]
13. Karlin, K.D.; Tyeklár, Z. (Eds.) *Bioinorganic Chemistry of Copper*; Chapman and Hall: New York, NY, USA, 1993.
14. Lubben, M.; Hage, R.; Meetsma, A.; Býma, K.; Fering, B.L. Modeling Dinuclear Copper Sites of Biological Relevance: Synthesis, Molecular Structure, Magnetic Properties, and ¹H NMR Spectroscopy of a Nonsymmetric Dinuclear Copper(II) Complex. Microcalorimetric Determination of Stepwise Complexation of Copper(II) by a Nonsymmetric Dinucleating Ligand. *Inorg. Chem.* **1995**, *34*, 2217–2224. [[CrossRef](#)]
15. Kitajima, N.; Fujisawa, K.; Fujimoto, C.; Morooka, Y.; Hashimoto, S.; Kitagawa, T.; Toriumi, K.; Tatsumi, K.; Nakamura, A. A new model for dioxygen binding in hemocyanin. Synthesis, characterization, and molecular structure of μ - η^2 : η^2 peroxo dinuclear copper(II) complexes, [Cu(HB(3,5-R₂pz)₃)₂(O₂)]₂ (R = *i*-Pr and Ph). *J. Am. Chem. Soc.* **1992**, *114*, 1277–1291. [[CrossRef](#)]

16. Fujieda, N.; Umakoshi, K.; Ochi, Y.; Nishikawa, Y.; Yanagisawa, S.; Kubo, M.; Kurisu, G.; Itoh, S. Copper–Oxygen Dynamics in the Tyrosinase Mechanism. *Angew. Chem. Int. Ed.* **2020**, *132*, 13487–13492. [[CrossRef](#)]
17. Ma, L.; Lu, L.; Zhu, M.; Wang, Q.; Gao, F.; Yuan, C.; Wu, Y.; Xing, S.; Fu, X.; Mei, Y.; et al. Dinuclear copper complexes of organic claw: Potent inhibition of protein tyrosine phosphatases. *J. Inorg. Biochem.* **2011**, *105*, 1138–1147. [[CrossRef](#)] [[PubMed](#)]
18. Neves, A.; Rossia, L.M.; Horn, A., Jr.; Vencato, I.; Bortoluzzi, A.J.; Zucco, C.; Mangrich, A.S. Synthesis, structure and properties of the first dinuclear copper(II) complex as a structural model for the phenolic intermediate in tyrosinase–cresolase activity. *Inorg. Chem. Commun.* **1999**, *2*, 334–337. [[CrossRef](#)]
19. Whittaker, J.W. *Metal Ions in Biological Systems*; Sigel, H., Sigel, A., Eds.; Marcel Dekker: New York, NY, USA, 1994; Volume 30, pp. 315–360.
20. Thomas, F.; Gellon, G.; Gautier-Luneau, I.; Saint-Aman, E.; Pierre, J.-L. A Structural and Functional Model of Galactose Oxidase: Control of the One-Electron Oxidized Active Form through Two Differentiated Phenolic Arms in a Tripodal Ligand. *Angew. Chem. Int. Ed.* **2002**, *41*, 3047–3050. [[CrossRef](#)]
21. Taki, M.; Kumei, H.; Nagatomo, S.; Kitagawa, T.; Itoh, S.; Fukuzumi, S. Active site models for galactose oxidase containing two different phenol groups. *Inorg. Chim. Acta* **2000**, *300–302*, 622–632. [[CrossRef](#)]
22. Sokolowski, A.; Leutbecher, H.; Weyhermüller, T.; Schnepf, R.; Bothe, E.; Bill, E.; Hildebrandt, P.; Wieghardt, K. Phenoxyl-copper(II) complexes: Models for the active site of galactose oxidase. *J. Biol. Inorg. Chem.* **1997**, *2*, 444–453. [[CrossRef](#)]
23. Ochs, C.; Hahn, F.E.; Fröhlich, R. Coordination Chemistry of Unsymmetrical Tripodal Ligands with NNO₂ Donor Set. *Eur. J. Inorg. Chem.* **2001**, 2427–2436. [[CrossRef](#)]
24. Ito, N.; Phillips, S.E.V.; Yadav, K.D.S.; Knowles, P.F. Crystal Structure of a Free Radical Enzyme, Galactose Oxidase. *J. Mol. Biol.* **1994**, *238*, 794–814. [[CrossRef](#)]
25. Mukherjee, D.; Nag, P.; Shteinman, A.A.; Vennapusa, S.R.; Mandal, U.; Mitra, M. Catechol oxidation promoted by bridging phenoxo moieties in a bis(μ -phenoxo)-bridged dicopper(II) complex. *RSC Adv.* **2021**, *11*, 22951–22959. [[CrossRef](#)]
26. Patriarca, M.; Daier, V.; Camí, G.; Rivière, E.; Hureau, C.; Signorella, S. Preparation, characterization and activity of CuZn and Cu² superoxide dismutase mimics encapsulated in mesoporous silica. *J. Inorg. Biochem.* **2020**, *207*, 111050. [[CrossRef](#)] [[PubMed](#)]
27. Biswas, A.; Das, L.K.; Drew, M.G.B.; Diaz, C.; Ghosh, A. Insertion of a Hydroxido Bridge into a Diphenoxido Dinuclear Copper(II) Complex: Drastic Change of the Magnetic Property from Strong Antiferromagnetic to Ferromagnetic and Enhancement in the Catecholase Activity. *Inorg. Chem.* **2012**, *51*, 10111–10121. [[CrossRef](#)] [[PubMed](#)]
28. Chen, Z.; Zhang, J.; Zhang, S. Oxidative DNA cleavage promoted by two phenolate-bridged binuclear copper(II) complexes. *New J. Chem.* **2015**, *39*, 1814–1821. [[CrossRef](#)]
29. Berthet, N.; Martel-Frchet, V.; Michel, F.; Philouze, C.; Hamman, S.; Ronot, X.; Thomas, F. Nuclease and anti-proliferative activities of copper(II) complexes of N₃O tripodal ligands involving a sterically hindered phenolate. *Dalton Trans.* **2013**, *42*, 8468–8483. [[CrossRef](#)]
30. Massoud, S.S.; Louka, F.R.; Salem, N.M.H.; Fischer, R.C.; Torvisco, A.; Mautner, F.A.; Vančo, J.; Belza, J.; Dvořák, Z.; Trávníček, Z. Dinuclear Doubly Bridged Phenoxido Copper(II) Complexes as Efficient Anticancer Agents. *Eur. J. Med. Chem.* **2023**, *246*, 114992. [[CrossRef](#)]
31. Jahromi, Z.M.; Asadi, Z.; Eigner, V.; Dusek, M.; Rastegari, B. A new phenoxo-bridged dicopper Schiff base complex: Synthesis, crystal structure DNA/BSA interaction, cytotoxicity assay and catecholase activity. *Polyhedron* **2022**, *221*, 115891. [[CrossRef](#)]
32. Ferrareso, L.G.; de Arruda, E.G.R.; de Moraes, T.P.L.; Fazzi, R.B.; Ferreira, A.M.D.C.; Abbehausen, C. Copper(II) and zinc(II) dinuclear enzymes model compounds: The nature of the metal ion in the biological function. *J. Mol. Struct.* **2017**, *1150*, 316–328. [[CrossRef](#)]
33. Novoa, N.; Justaud, F.; Hamon, P.; Roisnel, T.; Cador, O.; Guennic, B.L.; Manzur, C.; Carrillo, D.; Hamon, J.-R. Doubly phenoxide-bridged binuclear copper(II) complexes with ono tridentate Schiff base ligand: Synthesis, structural, magnetic and theoretical studies. *Polyhedron* **2015**, *86*, 81–88. [[CrossRef](#)]
34. Anbu, S.; Kandaswamy, M. Electrochemical, magnetic, catalytic, DNA binding and cleavage studies of new mono and binuclear copper(II) complexes. *Polyhedron* **2011**, *30*, 123–131. [[CrossRef](#)]
35. Assey, G.E.; Yisgedu, T.; Gultneh, Y.; Butcher, R.J.; Tesema, Y. Di- μ -perchlorato-bis- $\{\mu$ -2-[(2-pyrid-yl)methyl-amino-meth-yl]phenolato}dicopper(II) acetonitrile disolvate. *Acta Crystallogr. Sect. E Struct. Rep. Online* **2009**, *65*, m1007–m1008. [[CrossRef](#)]
36. Assey, G.E.; Tesema, Y.; Yisgedu, T.; Gultneh, Y.; Butcher, R.J. Bis[μ -2-(2-pyridylmethyl-amino-meth-yl)phenolato]- κ N,N',O:O; κ O:N,N',O-bis-[(thio-cyanato- κ N)copper(II)]. *Acta Crystallogr. Sect. E Struct. Rep. Online* **2009**, *65*, m1121–m1122. [[CrossRef](#)]
37. Ma, J.-C.; Yang, J.; Ma, J.-F. Bis[μ -2,4-dibromo-6-(2-pyridylmethylaminomethyl)phenolato]bis[nitratocopper(II)]. *Acta Crystallogr. Sect. E Struct. Rep. Online* **2007**, *63*, m2284. [[CrossRef](#)]
38. Choi, K.-Y. Synthesis and Crystal Structure of Phenolato-Bridged Dinuclear Copper(II) Complex with (2-Hydroxybenzyl)(2-pyridylmethyl)amine. *J. Chem. Cryst.* **2010**, *40*, 1016–1020. [[CrossRef](#)]
39. Tandon, S.S.; Bunge, S.D.; Patel, N.; Wang, E.C.; Thompson, L.K. Self-Assembly of Antiferromagnetically-Coupled Copper(II) Supramolecular Architectures with Diverse Structural Complexities. *Molecules* **2020**, *25*, 5549. [[CrossRef](#)]
40. Adams, H.; Bailey, N.A.; Campbell, I.K.; Fenton, D.E.; He, Q.-Y. Formation of axial phenolate–metal bonds in square-pyramidal complexes. *J. Chem. Soc. Dalton Trans.* **1996**, 2233–2237. [[CrossRef](#)]

41. Mallah, T.; Boillot, M.-L.; Kahn, O.; Gouteron, J.; Jeannin, S.; Jeannin, Y. Crystal Structures and Magnetic Properties of p-Phenolato Copper(II) Binuclear Complexes with Hydroxo, Azido, and Cyanato-O Exogenous Bridges. *Inorg. Chem.* **1986**, *25*, 3058–3065. [[CrossRef](#)]
42. You, X.; Wei, Z. Two multidentate ligands utilizing triazolyl, pyridinyl and phenolate groups as donors for constructing dinuclear copper(II) and iron(III) complexes: Syntheses, structures, and electrochemistry. *Inorg. Chim. Acta* **2014**, *423*, 332–339. [[CrossRef](#)]
43. Rajendiran, T.M.; Kannappan, R.; Mahalakshmy, R.; Rajeswari, J.; Venkatesan, R.; Rao, P. New unsymmetrical μ -phenoxo-bridged binuclear copper(II) complexes. *Transit. Met. Chem.* **2003**, *28*, 447–454. [[CrossRef](#)]
44. Manzur, J.; Mora, H.; Vega, A.; Spodine, E.; Venegas-Yazigi, D.; Garland, M.T.; El Fallah, M.S.; Escuer, A. Copper(II) complexes with new polypodal ligands presenting axial–equatorial phenoxo bridges {2-[(bis(2-pyridylmethyl)amino)methyl]-4-methylphenol, 2-[(bis(2-pyridylmethyl)amino)methyl]-4-methyl-6-(methylthio)phenol]: Examples of ferromagnetically coupled bi- and trinuclear copper(II) complexes. *Inorg. Chem.* **2007**, *46*, 6924–6932. [[CrossRef](#)]
45. Kani, Y.; Ohba, S.; Ito, S.; Nishida, Y. Redetermination of bis[[2-(hydroxyphenylmethyl)bis(2-pyridylmethyl)aminato]copper(II)]diperchlorate. *Acta Crystallogr. Sect. C Cryst. Struct. Commun.* **2000**, *56*, e201. [[CrossRef](#)] [[PubMed](#)]
46. Michel, F.; Torelli, S.; Thomas, F.; Duboc, C.; Philouze, C.; Belle, C.; Hamman, S.; Aman, E.S.; Pierre, J.-L. An Unprecedented Bridging Phenoxyl Radical in Dicopper(II) Complexes: Evidence for an $S = 3/2$ Spin State. *Angew. Chem. Int. Ed.* **2005**, *44*, 438–441. [[CrossRef](#)]
47. Philibert, A.; Thomas, F.; Philouze, C.; Hamman, S.; Saint-Aman, E.; Pierre, J.-L. Galactose Oxidase Models: Tuning the Properties of CuII-Phenoxy Radicals. *Chem. Eur. J.* **2003**, *9*, 3803–3812. [[CrossRef](#)]
48. Wendt, F.; Rolff, M.; Thimm, W.; Näther, C.; Tuzcek, F. A Small-molecule Model System of Galactose Oxidase: Geometry, Reactivity, and Electronic Structure. *Z. Anorg. Allg. Chem.* **2013**, *639*, 2502–2509. [[CrossRef](#)]
49. Taki, M.; Hattori, H.; Osako, T.; Nagatomo, S.; Shiro, M.; Kitagawa, T.; Itoh, S. Model complexes of the active site of galactose oxidase. Effects of the metal ion binding sites. *Inorg. Chim. Acta* **2004**, *357*, 3369–3381. [[CrossRef](#)]
50. Yajima, T.; Shimazaki, Y.; Ishigami, N.; Odani, A.; Yamauchi, O. Conformational preference of the side chain aromatic ring in Cu(II) and Pd(II) complexes of 2N1O-donor ligands. *Inorg. Chim. Acta* **2002**, *337*, 193–202. [[CrossRef](#)]
51. Vaidyanathan, M.; Viswanathan, R.; Palaniandavar, M.; Balasubramanian, T.; Prabhakaran, P.; Muthiah, T.P. Copper(II) Complexes with Unusual Axial Phenolate Coordination as Structural Models for the Active Site in Galactose Oxidase: X-ray Crystal Structures and Spectral and Redox Properties of [Cu(bnpn)X] Complexes. *Inorg. Chem.* **1998**, *37*, 6418–6427. [[CrossRef](#)]
52. Banerjee, I.; Dolai, M.; Jana, A.D.; Das, K.K.; Ali, M. σ -Aromaticity in dinuclear copper(ii) complexes: Novel interaction between perchlorate anion and σ -aromatic [Cu₂X₂] (X = N or O) core. *CrystEngComm* **2012**, *14*, 4972–4975. [[CrossRef](#)]
53. Thompson, L.K.; Mandal, S.K.; Tandon, S.S.; Bridson, J.N.; Park, M.K. Magnetostructural Correlations in Bis(μ 2-phenoxide)-Bridged Macrocyclic Dinuclear Copper(II) Complexes. Influence of Electron-Withdrawing -Withdrawing Substituents on Exchange Coupling. *Inorg. Chem.* **1996**, *35*, 3117–3125. [[CrossRef](#)]
54. Yadav, A.; Lama, P.; Bieńko, A.; Bieńko, D.; Siddiqui, K.A. H-bonded supramolecular synthon induced magnetic superexchange phenomenon results weak ferromagnetic and strong antiferromagnetic interactions in two new copper-oxalate coordination network. *Polyhedron* **2018**, *141*, 247–261. [[CrossRef](#)]
55. Tang, J.; Costa, J.S.; Golobič, A.; Kozlečvar, B.; Robertazzi, A.; Vargiu, A.V.; Gamez, P.; Reedijk, J. Magnetic Coupling between Copper(II) Ions Mediated by Hydrogen-Bonded (Neutral) Water Molecules. *Inorg. Chem.* **2009**, *48*, 5473–5479. [[CrossRef](#)] [[PubMed](#)]
56. Biswas, C.; Drew, M.G.B.; Asthana, S.; Desplanches, C.; Ghosh, A. Mono-aqua-bridged dinuclear complexes of Cu(II) containing NNO donor Schiff base ligand: Hydrogen-bond-mediated exchange coupling. *J. Mol. Struct.* **2010**, *965*, 39–44. [[CrossRef](#)]
57. Talukder, P.; Sen, S.; Mitra, S.; Dahlenberg, L.; Desplanches, C.; Sutter, J.-P. Evidence for Hydrogen-Bond-Mediated Exchange Coupling in an Aqua-Bridged CuII Dimer: Synthesis, Magnetic Study and Correlation with Density Functional Calculations. *Eur. J. Inorg. Chem.* **2006**, *2006*, 329–333. [[CrossRef](#)]
58. Okazawa, A.; Ishida, T. Super–superexchange coupling through a hydrogen bond in a linear copper(II) complex, [Cu(LH)(L)]·BF₄·2H₂O (LH = N-tert-butyl-N-2-pyridylhydroxylamine). *Chem. Phys. Lett.* **2009**, *480*, 198–202. [[CrossRef](#)]
59. Valigura, D.; Moncol, J.; Korabik, M.; Pucekova, Z.; Lis, T.; Mrozinski, J.; Melnik, M. New Dimeric Copper(II) Complex [Cu(5-MeOsal)₂(μ -nia)(H₂O)]₂ with Magnetic Exchange Interactions through H-Bonds. *Eur. J. Inorg. Chem.* **2006**, 3813–3817. [[CrossRef](#)]
60. Desplanches, C.; Ruiz, E.; Rodriguez-Forteza, A.; Alvarez, S. Exchange Coupling of Transition-Metal Ions through Hydrogen Bonding: A Theoretical Investigation. *J. Am. Chem. Soc.* **2002**, *124*, 5197–5205. [[CrossRef](#)]
61. Plass, W.; Pohlmann, A.; Rautengarten, J. Magnetic Interactions as Supramolecular Function: Structure and Magnetic Properties of Hydrogen-Bridged Dinuclear Copper(II) Complexes. *Angew. Chem. Int. Ed.* **2001**, *40*, 4207–4210. [[CrossRef](#)]
62. Moreno, J.M.; Ruiz, J.; Dominguez-Vera, J.M.; Colacio, E. Spectroscopic and magnetic properties, and crystal structure of a dimer copper(II) complex via hydrogen bonding with a weak ferromagnetic interaction. *Inorg. Chim. Acta* **1993**, *208*, 111–115. [[CrossRef](#)]
63. Colacio, E.; Costes, J.P.; Kivekas, R.; Laurent, J.P.; Ruiz, J.; Sundberg, M. A new hydrogen-bonded dinuclear complex involving copper(II) ions in a pseudotetrahedral N₃O environment: Molecular and crystal structure and magnetic and spectroscopic properties. *Inorg. Chem.* **1991**, *30*, 1475–1479. [[CrossRef](#)]

64. Oberhausen, K.J.; Richardson, J.F.; Buchanan, R.M.; McCusker, J.K.; Hendrickson, D.N.; Latour, J.M. Synthesis and characterization of dinuclear copper(II) complexes of the dinucleating ligand 2,6-bis[bis((1-methylimidazol-2-yl)methyl)amino]methyl]-4-methylphenol. *Inorg. Chem.* **1991**, *30*, 1357–1365. [[CrossRef](#)]
65. Mautner, F.A.; Fischer, R.C.; Rashmawi, L.G.; Louka, F.R.; Massoud, S.S. Structural characterization of metal(II) thiocyanato complexes derived from bis(2-(H-pyrazol-1-yl)ethyl)amine. *Polyhedron* **2017**, *124*, 237–242. [[CrossRef](#)]
66. Massoud, S.S.; Louka, R.F.; David, R.N.; Dartez, M.J.; Nguyn, Q.L.; Labry, N.J.; Fischer, R.C.; Mautner, F.A. Five-coordinate metal(II) complexes based pyrazolyl ligands. *Polyhedron* **2015**, *90*, 258–265. [[CrossRef](#)]
67. Geary, W.J. The use of conductivity measurements in organic solvents for the characterisation of coordination compounds. *Coord. Chem. Rev.* **1971**, *7*, 81–122. [[CrossRef](#)]
68. Addison, A.W.; Rao, T.N.; Reedijk, J.; Rijn, J.V.; Verschoor, G.C. Synthesis, structure, and spectroscopic properties of copper(II) compounds containing nitrogen–sulphur donor ligands; the crystal and molecular structure of aqua[1,7-bis(N-methylbenzimidazol-2'-yl)-2,6-dithiaheptane]copper(II) perchlorate. *J. Chem. Soc. Dalton Trans.* **1984**, 1349–1356. [[CrossRef](#)]
69. Archana, V.; Imamura, Y.; Sakiyama, H.; Hada, M. Correlating Magnetic Exchange in Dinuclear Bis(phenolate)-Bridged Complexes: A Computational Perspective. *Bull. Chem. Soc. Jpn. (BCSJ)* **2016**, *89*, 657–665. [[CrossRef](#)]
70. Venegas-Yazigi, D.; Aravena, D.; Spodine, E.; Ruiz, E.; Alvarez, S. Structural and electronic effects on the exchange interactions in dinuclear bis(phenoxo)-bridged copper(II) complexes. *Coord. Chem. Rev.* **2010**, *254*, 2086–2095. [[CrossRef](#)]
71. Mondal, D.; Majee, M.C.; Bhattacharya, K.; Long, J.; Larionova, J.; Khusniyarov, M.M.; Chaudhury, M. Crossover from Antiferromagnetic to Ferromagnetic Exchange Coupling in a New Family of Bis-(μ -phenoxido)dicopper(II) Complexes: A Comprehensive Magneto-Structural Correlation by Experimental and Theoretical Study. *ACS Omega* **2019**, *4*, 10558–10570. [[CrossRef](#)]
72. Mondal, D.; Majee, M.C.; Bhattacharya, K.; Long, J.; Larionova, J.; Khusniyarov, M.M.; Chaudhury, M. Synthesis and characterization of binuclear [ONOX]-type amine-bis(phenolate) copper(II) complexes. *Inorg. Chim. Acta* **2011**, *375*, 158–165.
73. Chaudhuri, P.; Wagner, R.; Weyhermüller, T. Ferromagnetic vs. antiferromagnetic coupling in bis(μ -phenoxo)dicopper(II) complexes. Tuning of the nature of exchange coupling by remote ligand substituents. *Inorg. Chem.* **2007**, *46*, 5134–5136. [[CrossRef](#)] [[PubMed](#)]
74. Van Crawford, H.; Richardson, H.W.; Wasson, J.R.; Hodgson, D.J.; Hatfield, W.E. Relation between the singlet-triplet splitting and the copper-oxygen-copper bridge angle in hydroxo-bridged copper dimers. *Inorg. Chem.* **1976**, *15*, 2107–2110. [[CrossRef](#)]
75. Merz, L.; Hasse, W. Exchange interaction in tetrameric oxygen-bridged copper clusters of the cubane type. *Dalton Trans.* **1980**, 875–879. [[CrossRef](#)]
76. Kahn, O. *Molecular Magnetism*; VCH: Cambridge, UK, 1993; Chapter 1.
77. Bruker. *SAINT*, version 7.23; Bruker: Billerica, MA, USA, 2005.
78. Bruker. *APEX 2*, version 2.0-2; Bruker: Billerica, MA, USA, 2006.
79. Sheldrick, G.M. *SADABS*, version 2; University of Goettingen: Goettingen, Germany, 2001.
80. Sheldrick, G.M. A short history of SHELX. *Acta Crystallogr. A* **2008**, *64*, 112–122. [[CrossRef](#)]
81. Sheldrick, G.M. Crystal structure refinement with SHELXL. *Acta Crystallogr. C* **2015**, *71*, 3–5. [[CrossRef](#)] [[PubMed](#)]
82. Macrae, C.F.; Edington, P.R.; McCabe, P.; Pidcock, E.; Shields, G.P.; Taylor, R.; Towler, T.; van de Streek, J.J. Mercury: Visualization and analysis of crystal structures. *J. Appl. Cryst.* **2006**, *39*, 453–457. [[CrossRef](#)]
83. Speck, A.L. *PLATON, a Multipurpose Crystallographic Tool*; Utrecht University: Utrecht, The Netherlands, 2001.

Disclaimer/Publisher’s Note: The statements, opinions and data contained in all publications are solely those of the individual author(s) and contributor(s) and not of MDPI and/or the editor(s). MDPI and/or the editor(s) disclaim responsibility for any injury to people or property resulting from any ideas, methods, instructions or products referred to in the content.